

Correlation Dynamics of Yukawa-theory in 1+1 dimensions*

S. Juchem, W. Cassing and J.M. Häuser
Institut für Theoretische Physik, Universität Gießen
35392 Gießen, Germany

August 14, 2018

Abstract

Using the method of correlation dynamics we investigate the properties of a field-theory for fermions and scalar bosons coupled via a Yukawa interaction. Within this approach, which consists in an expansion of full equal-time Green functions into connected equal-time Green functions and a corresponding truncation of the hierarchy of equations of motion we carry out calculations up to 4th order in the connected Green functions and evaluate the effective potential of the theory in 1+1 dimensions on a torus. Comparing the different approximations we find a strong influence of the connected 4-point functions on the properties of the system.

*supported by DFG, GSI Darmstadt

1 Introduction

Up to now the problem of strongly interacting fermion and boson field-theories is not solved in a satisfying manner and there is a need for nonperturbative approximation schemes. In the last decades many non-perturbative approaches were developed such as variational methods [1, 2], Dyson-Schwinger-calculations [3, 4] or the coupled cluster expansion [5, 6]. Among the approaches that are based on techniques known from many-particle physics is the method of correlation dynamics, which was successfully applied to the nonrelativistic nuclear many-particle problem [7, 8, 9] and for the description of interacting boson systems [10]. Within a formulation in terms of connected equal-time Green functions the problem of ground-state symmetry breaking was studied in detail for Φ^4 -theory in $1 + 1$ and $2 + 1$ space-time dimensions [11, 12] as well as the convergence properties of the truncation scheme applied [13]. In this article the correlation dynamical approach is extended from a pure boson theory to a field theory containing both bosonic and fermionic degrees of freedom, i.e. Yukawa-theory in $1 + 1$ space-time dimensions.

The paper is organized as follows: In Section 2 we present the connected Green function approach for Yukawa-theory in $1 + 1$ space-time dimensions and discuss the correlation dynamical hierarchy for connected equal-time Green functions in different truncation schemes. Furtheron, we study the divergence structure of the Yukawa-theory in $1 + 1$ dimensions and renormalize as in a comparable Gaussian-Effective-Potential-(GEP)-approach [14]. In Section 3 we show the results obtained in our numerical calculations for different truncation schemes up to the level of connected 4-point functions. A summary is given in Section 4 while the Appendices contain the higher order cluster expansions and all correlation dynamical equations of motion up to fourth order.

2 Correlation dynamics of Yukawa-theory

2.1 The equations of motion for connected equal-time Green functions

In the present work we investigate the Yukawa-theory in $1 + 1$ space-time dimensions given by the Lagrangian,

$$\mathcal{L} = \frac{1}{2}\partial_\mu\Phi\partial^\mu\Phi - \frac{1}{2}m_B^2\Phi^2 + \bar{\Psi}(i\gamma^\mu\partial_\mu - M_B)\Psi - g_B\bar{\Psi}\Psi\Phi, \quad (1)$$

or the Hamiltonian density,

$$\mathcal{H} = \frac{1}{2}\Pi^2 + \frac{1}{2}(\vec{\nabla}\Phi)^2 + \frac{1}{2}m_B^2\Phi^2 + \bar{\Psi}(-i\vec{\gamma}\vec{\nabla} + M_B)\Psi + g_B\bar{\Psi}\Psi\Phi. \quad (2)$$

Here m_B and M_B denote the bare masses of the boson and the fermion fields, respectively, while g_B represents the bare Yukawa-coupling. The fields themselves have to

be considered as bare fields where we have dropped the corresponding indices. They fulfill equal-time commutation relations for the boson fields

$$[\Phi(\vec{x}, t), \Pi(\vec{y}, t)] = i \delta^{(\nu)}(\vec{x} - \vec{y}), \quad (3)$$

$$[\Phi(\vec{x}, t), \Phi(\vec{y}, t)] = [\Pi(\vec{x}, t), \Pi(\vec{y}, t)] = 0 \quad (4)$$

and equal-time anticommutation relations for the fermion fields

$$\{\bar{\Psi}_a(\vec{x}, t), \Psi_b(\vec{y}, t)\} = \gamma_{ab}^0 \delta^{(\nu)}(\vec{x} - \vec{y}), \quad (5)$$

$$\{\bar{\Psi}_a(\vec{x}, t), \bar{\Psi}_b(\vec{y}, t)\} = \{\Psi_a(\vec{x}, t), \Psi_b(\vec{y}, t)\} = 0, \quad (6)$$

where a and b denote the components of the spinor. Making use of these relations one obtains the time evolution of any operator \hat{O} via the Heisenberg equation

$$i\partial_t \hat{O} = [\hat{O}, H]. \quad (7)$$

The equations of motion for the field operators read:

$$\partial_t \Phi(\vec{x}) = \Pi(\vec{x}), \quad (8)$$

$$\partial_t \Pi(\vec{x}) = (\vec{\nabla}_x^2 - m_B^2) \Phi(\vec{x}) - g_B \bar{\Psi}_l(\vec{x}) \Psi_l(\vec{x}), \quad (9)$$

$$\partial_t \bar{\Psi}_a(\vec{x}) = \bar{\alpha}_{la} \vec{\nabla}_x \bar{\Psi}_l(\vec{x}) + iM_B \beta_{la} \bar{\Psi}_l(\vec{x}) + ig_B \beta_{la} \bar{\Psi}_l(\vec{x}) \Phi(\vec{x}), \quad (10)$$

$$\partial_t \Psi_b(\vec{x}) = -\bar{\alpha}_{bl} \vec{\nabla}_x \Psi_l(\vec{x}) - iM_B \beta_{bl} \Psi_l(\vec{x}) - ig_B \beta_{bl} \Psi_l(\vec{x}) \Phi(\vec{x}),$$

where all operators are considered at the same time t which is suppressed in our notation. In 1+1 dimensions the Dirac-matrices are given by the representation

$$\beta = \gamma^0 = \begin{pmatrix} 1 & 0 \\ 0 & -1 \end{pmatrix}, \quad \alpha^1 = \begin{pmatrix} 0 & 1 \\ 1 & 0 \end{pmatrix}, \quad \gamma^1 = \beta \alpha^1 = \begin{pmatrix} 0 & 1 \\ -1 & 0 \end{pmatrix}. \quad (11)$$

For any arbitrary product of these field operators the time evolution is obtained correspondingly. The boson field momentum Π is considered explicitly in order to end up with equations of motion of first order in time. Due to the Yukawa-coupling term the time evolution of any field operator product, which consists at least of two fermion fields or one boson field momentum, is influenced by field operator products of the next higher order.

By taking the expectation value of these operator identities we end up with an infinite hierarchy of equations of motion for equal-time Green functions which is equivalent

to the BBGKY¹-density-matrix-hierarchy of ordinary many-body physics [15]. For the lowest orders we find:

$$\partial_t \langle \Phi(\vec{x}_1)\Phi(\vec{x}_2) \rangle = \langle \Pi(\vec{x}_1)\Phi(\vec{x}_2) \rangle + \langle \Phi(\vec{x}_1)\Pi(\vec{x}_2) \rangle, \quad (12)$$

$$\begin{aligned} \partial_t \langle \Pi(\vec{x}_1)\Phi(\vec{x}_2) \rangle &= (\vec{\nabla}_{x_1}^2 - m_B^2) \langle \Phi(\vec{x}_1)\Phi(\vec{x}_2) \rangle + \langle \Pi(\vec{x}_1)\Pi(\vec{x}_2) \rangle \\ &\quad - g_B \langle \bar{\Psi}_l(\vec{x}_1)\Psi_l(\vec{x}_1)\Phi(\vec{x}_2) \rangle, \end{aligned} \quad (13)$$

$$\begin{aligned} \partial_t \langle \Pi(\vec{x}_1)\Pi(\vec{x}_2) \rangle &= (\vec{\nabla}_{x_1}^2 - m_B^2) \langle \Phi(\vec{x}_1)\Pi(\vec{x}_2) \rangle + (\vec{\nabla}_{x_2}^2 - m_B^2) \langle \Pi(\vec{x}_1)\Phi(\vec{x}_2) \rangle \\ &\quad - g_B \langle \bar{\Psi}_l(\vec{x}_1)\Psi_l(\vec{x}_1)\Pi(\vec{x}_2) \rangle - g_B \langle \bar{\Psi}_l(\vec{x}_2)\Psi_l(\vec{x}_2)\Pi(\vec{x}_1) \rangle, \end{aligned} \quad (14)$$

$$\begin{aligned} \partial_t \langle \bar{\Psi}_a(\vec{x}_1)\Psi_b(\vec{x}_2) \rangle &= \vec{\alpha}_{la}\vec{\nabla}_{x_1} \langle \bar{\Psi}_l(\vec{x}_1)\Psi_b(\vec{x}_2) \rangle - \vec{\alpha}_{bl}\vec{\nabla}_{x_2} \langle \bar{\Psi}_a(\vec{x}_1)\Psi_l(\vec{x}_2) \rangle \\ &\quad + iM_B\beta_{la} \langle \bar{\Psi}_l(\vec{x}_1)\Psi_b(\vec{x}_2) \rangle - iM_B\beta_{bl} \langle \bar{\Psi}_a(\vec{x}_1)\Psi_l(\vec{x}_2) \rangle \\ &\quad + ig_B\beta_{la} \langle \bar{\Psi}_l(\vec{x}_1)\Psi_b(\vec{x}_2)\Phi(\vec{x}_1) \rangle \\ &\quad - ig_B\beta_{bl} \langle \bar{\Psi}_a(\vec{x}_1)\Psi_l(\vec{x}_2)\Phi(\vec{x}_2) \rangle. \end{aligned} \quad (15)$$

In order to solve this infinite set of equations a truncation scheme must be applied. The ansatz of correlation dynamics consists of two steps: i) all full equal-time Green functions are replaced by sums of products of connected equal-time Green functions via a cluster expansion, which leads to a – still infinite – hierarchy for the connected Green functions, ii) a truncation scheme is applied to this hierarchy by neglecting all connected equal-time Green functions of order $n > N$. This closed set of equations of motion for connected equal-time Green functions is denoted as the *correlation dynamical N-point approximation*.

Before deriving this set for the Yukawa-theory we separate the classical part from the boson field, since here we are primarily interested in the effective potential of the theory. The boson field is written as

$$\Phi = \Phi_0 + \hat{\Phi}, \quad (16)$$

where Φ_0 is the classical contribution given by $\langle \Phi \rangle = \Phi_0$ and $\hat{\Phi}$ the pure quantum mechanical part with vanishing expectation value $\langle \hat{\Phi} \rangle = 0$. With this separation the effective potential of the field theory is equivalent to the minimal energy density in the subspace of fixed vacuum expectation value Φ_0 , i.e.

$$V_{\text{eff}}(\Phi_0) = \min_{\{\Xi\}} \langle \Xi | \mathcal{H} | \Xi \rangle, \quad \text{with} \quad \langle \Xi | \Phi | \Xi \rangle = \Phi_0, \quad \langle \Xi | \Xi \rangle = 1. \quad (17)$$

Using (16) the modified Lagrangian reads

$$\mathcal{L} = \frac{1}{2} \partial_\mu \hat{\Phi} \partial^\mu \hat{\Phi} - \frac{1}{2} m_B^2 (\hat{\Phi} + \Phi_0)^2 + \bar{\Psi}(i\gamma^\mu \partial_\mu - M_B - g_B \Phi_0)\Psi - g_B \bar{\Psi}\Psi\hat{\Phi}, \quad (18)$$

¹Bogoliubov-Born-Green-Kirkwood-Yvon

and the corresponding Hamiltonian density is given by

$$\mathcal{H} = \frac{1}{2}\hat{\Pi}^2 + \frac{1}{2}(\vec{\nabla}\hat{\Phi})^2 + \frac{1}{2}m_B^2(\hat{\Phi} + \Phi_0)^2 + \bar{\Psi}(-i\vec{\gamma}\vec{\nabla} + M_B + g_B\Phi_0)\Psi + g_B\bar{\Psi}\Psi\hat{\Phi}. \quad (19)$$

Since we take Φ_0 to be fixed, i.e. $\partial_t\Phi_0 = 0$, we have $\Pi = \partial_t\Phi = \partial_t\hat{\Phi} = \hat{\Pi}$. As a consequence the Hamiltonian density now contains a contribution which is generated by the interaction part and has the same structure as the fermion mass term. The modified equations of motion for the full equal-time Green functions are obtained by replacing M_B by $M_B + g_B\Phi_0$ and the boson field Φ by its quantum part $\hat{\Phi}$.

The cluster expansion is derived from the relation between the generating functionals of full and connected Green functions and by taking the well defined equal-time limit. For the bosonic case this is presented in detail in Ref. [11] in context of Φ^4 -theory and thus will not be repeated here. We only show the expansion for the lowest order boson Green functions (with field operators $\hat{O}_i(\vec{x}_i) \in \{\Phi(\vec{x}_i), \Pi(\vec{x}_i)\}$):

$$\langle \hat{O}_1(\vec{x}_1) \rangle = \langle \hat{O}_1(\vec{x}_1) \rangle_c, \quad (20)$$

$$\langle \hat{O}_1(\vec{x}_1) \hat{O}_2(\vec{x}_2) \rangle = \langle \hat{O}_1(\vec{x}_1) \hat{O}_2(\vec{x}_2) \rangle_c + \langle \hat{O}_1(\vec{x}_1) \rangle_c \langle \hat{O}_2(\vec{x}_2) \rangle_c, \quad (21)$$

$$\begin{aligned} \langle \hat{O}_1(\vec{x}_1) \hat{O}_2(\vec{x}_2) \hat{O}_3(\vec{x}_3) \rangle &= \langle \hat{O}_1(\vec{x}_1) \hat{O}_2(\vec{x}_2) \hat{O}_3(\vec{x}_3) \rangle_c \\ &+ \langle \hat{O}_1(\vec{x}_1) \hat{O}_2(\vec{x}_2) \rangle_c \langle \hat{O}_3(\vec{x}_3) \rangle_c + \langle \hat{O}_1(\vec{x}_1) \hat{O}_3(\vec{x}_3) \rangle_c \langle \hat{O}_2(\vec{x}_2) \rangle_c \\ &+ \langle \hat{O}_2(\vec{x}_2) \hat{O}_3(\vec{x}_3) \rangle_c \langle \hat{O}_1(\vec{x}_1) \rangle_c + \langle \hat{O}_1(\vec{x}_1) \rangle_c \langle \hat{O}_2(\vec{x}_2) \rangle_c \langle \hat{O}_3(\vec{x}_3) \rangle_c. \end{aligned} \quad (22)$$

In the fermionic sector the source terms appearing in the generating functionals are anticommuting Grassmann fields. Thus the cluster expansions differ from the boson case and read in the lowest orders:

$$\langle \bar{\Psi}(\vec{x}_1) \Psi(\vec{x}_2) \rangle = \langle \bar{\Psi}(\vec{x}_1) \Psi(\vec{x}_2) \rangle_c, \quad (23)$$

$$\begin{aligned} \langle \bar{\Psi}(\vec{x}_1) \bar{\Psi}(\vec{x}_2) \Psi(\vec{x}_3) \Psi(\vec{x}_4) \rangle &= \langle \bar{\Psi}(\vec{x}_1) \bar{\Psi}(\vec{x}_2) \Psi(\vec{x}_3) \Psi(\vec{x}_4) \rangle_c \\ &+ \langle \bar{\Psi}(\vec{x}_1) \Psi(\vec{x}_4) \rangle_c \langle \bar{\Psi}(\vec{x}_2) \Psi(\vec{x}_3) \rangle_c \\ &- \langle \bar{\Psi}(\vec{x}_1) \Psi(\vec{x}_3) \rangle_c \langle \bar{\Psi}(\vec{x}_2) \Psi(\vec{x}_4) \rangle_c. \end{aligned} \quad (24)$$

Due to the absence of fermionic n-point functions of odd order the full and the connected 2-point function are equivalent. Therefore the index \cdot_c for the connected Green functions can be dropped for $\langle \bar{\Psi}\Psi \rangle$ as in case of the boson 1-point function. For the mixed 3-point functions we find:

$$\begin{aligned} \langle \bar{\Psi}(\vec{x}_1) \Psi(\vec{x}_2) \hat{O}_3(\vec{x}_3) \rangle &= \langle \bar{\Psi}(\vec{x}_1) \Psi(\vec{x}_2) \hat{O}_3(\vec{x}_3) \rangle_c \\ &+ \langle \bar{\Psi}(\vec{x}_1) \Psi(\vec{x}_2) \rangle_c \langle \hat{O}_3(\vec{x}_3) \rangle; \end{aligned} \quad (25)$$

the higher orders up to the 5-point-level are given in Appendix A.

An insertion of the cluster expansions into the hierarchy of equations of motion for full equal-time Green functions leads to a corresponding hierarchy for connected equal-time Green functions. In the present work three different truncation prescriptions are applied to this coupled set of equations, i.e. including all connected equal-time Green functions up to the 2-point-, the 3-point- and the 4-point-level. These approximations are denoted as $Y_{1+1}CD(2)$ -, $Y_{1+1}CD(3)$ - and $Y_{1+1}CD(4)$ -approximation. As examples for the equations of motion for connected equal-time Green functions we present those of lowest order:

$$\partial_t \langle \hat{\Phi}(\vec{x}_1) \hat{\Phi}(\vec{x}_2) \rangle_c = \langle \hat{\Pi}(\vec{x}_1) \hat{\Phi}(\vec{x}_2) \rangle_c + \langle \hat{\Phi}(\vec{x}_1) \hat{\Pi}(\vec{x}_2) \rangle_c, \quad (26)$$

$$\begin{aligned} \partial_t \langle \hat{\Pi}(\vec{x}_1) \hat{\Phi}(\vec{x}_2) \rangle_c &= t(\vec{x}_1) \langle \hat{\Phi}(\vec{x}_1) \hat{\Phi}(\vec{x}_2) \rangle_c + \langle \hat{\Pi}(\vec{x}_1) \hat{\Pi}(\vec{x}_2) \rangle_c \\ &\quad - g_B \langle \bar{\Psi}_l(\vec{x}_1) \Psi_l(\vec{x}_1) \hat{\Phi}(\vec{x}_2) \rangle_c, \end{aligned} \quad (27)$$

$$\begin{aligned} \partial_t \langle \hat{\Pi}(\vec{x}_1) \hat{\Pi}(\vec{x}_2) \rangle_c &= t(\vec{x}_1) \langle \hat{\Phi}(\vec{x}_1) \hat{\Pi}(\vec{x}_2) \rangle_c + t(\vec{x}_2) \langle \hat{\Pi}(\vec{x}_1) \hat{\Phi}(\vec{x}_2) \rangle_c \\ &\quad - g_B \langle \bar{\Psi}(\vec{x}_1) \Psi(\vec{x}_1) \hat{\Pi}(\vec{x}_2) \rangle_c - g_B \langle \bar{\Psi}(\vec{x}_2) \Psi(\vec{x}_2) \hat{\Pi}(\vec{x}_1) \rangle_c, \end{aligned} \quad (28)$$

$$\begin{aligned} \partial_t \langle \bar{\Psi}_a(\vec{x}_1) \Psi_b(\vec{x}_2) \rangle_c &= \tilde{t}(\vec{x}_1)_{la} \langle \bar{\Psi}_l(\vec{x}_1) \Psi_b(\vec{x}_2) \rangle_c - \tilde{t}(\vec{x}_2)_{lb} \langle \bar{\Psi}_a(\vec{x}_1) \Psi_l(\vec{x}_2) \rangle_c \\ &\quad + ig_B \beta_{la} \langle \bar{\Psi}_l(\vec{x}_1) \Psi_b(\vec{x}_2) \hat{\Phi}(\vec{x}_1) \rangle_c \\ &\quad - ig_B \beta_{bl} \langle \bar{\Psi}_a(\vec{x}_1) \Psi_l(\vec{x}_2) \hat{\Phi}(\vec{x}_2) \rangle_c, \end{aligned} \quad (29)$$

where the connected 3-point functions are neglected in the limit $Y_{1+1}CD(2)$. In (27)-(29) the following operators have been introduced for the bosonic part

$$t(\vec{x}) := (\vec{\nabla}_x^2 - m_B^2) \quad (30)$$

and the fermionic part

$$\tilde{t}(\vec{x})_{ab} := \vec{\alpha}_{ab} \vec{\nabla}_x + i(M_B + g_B \Phi_0) \beta_{ab}. \quad (31)$$

With regard to a numerical treatment we expand all field operators in a basis of orthonormal single-particle wavefunctions. Here we use a set of plane waves in a box of size L with periodic boundary conditions. This choice allows for an explicit exploitation of the translational invariance of the theory. The expansion of the field operators is given by:

$$\begin{aligned} \hat{\Phi}(\vec{x}) &= \sum_{\alpha} \varphi_{\alpha} \chi_{\alpha}(\vec{x}), \\ \hat{\Pi}(\vec{x}) &= \sum_{\alpha} \pi_{\alpha} \chi_{\alpha}(\vec{x}), \\ \bar{\Psi}_a(\vec{x}) &= \sum_{\alpha} \bar{\psi}_{a\alpha} \chi_{\alpha}(\vec{x}), \\ \Psi_b(\vec{x}) &= \sum_{\alpha} \psi_{b\alpha} \chi_{\alpha}(\vec{x}), \end{aligned} \quad (32)$$

where the elements of the single-particle basis χ_α obey the following orthonormality relations in $\nu + 1$ space-time dimensions:

$$\int d^\nu x \chi_\alpha^*(\vec{x}) \chi_\beta(\vec{x}) = \delta_{\alpha\beta}. \quad (33)$$

The greek indices refer to the basis elements and the latin indices represent the spinor components in (32). One straightforwardly obtains the equations of motion for the expansion coefficients of the connected equal-time Green functions. Introducing the abbreviations

$$\langle \alpha | \lambda_1 \lambda_2 \rangle = \int d^\nu x \chi_\alpha^*(\vec{x}) \chi_{\lambda_1}(\vec{x}) \chi_{\lambda_2}(\vec{x}), \quad (34)$$

$$\begin{aligned} t_{\alpha\beta} &= \int d^\nu x \chi_\alpha^*(\vec{x}) \left[\vec{\nabla}_x^2 - m_B^2 \right] \chi_\beta(\vec{x}) \\ &= \int d^\nu x \chi_\alpha^*(\vec{x}) t(\vec{x}) \chi_\beta(\vec{x}), \end{aligned} \quad (35)$$

$$\begin{aligned} \tilde{t}_{\alpha\beta}^{ab} &= \int d^\nu x \chi_\alpha^*(\vec{x}) \left[\vec{\alpha}_{ab} \vec{\nabla}_x + i(M_B + g_B \Phi_0) \beta_{ab} \right] \chi_\beta(\vec{x}) \\ &= \int d^\nu x \chi_\alpha^*(\vec{x}) \tilde{t}_{ab}(\vec{x}) \chi_\beta(\vec{x}), \end{aligned} \quad (36)$$

they read in lowest order:

$$\partial_t \langle \varphi_\alpha \varphi_\beta \rangle_c = \langle \pi_\alpha \varphi_\beta \rangle_c + \langle \varphi_\alpha \pi_\beta \rangle_c, \quad (37)$$

$$\begin{aligned} \partial_t \langle \pi_\alpha \varphi_\beta \rangle_c &= \langle \pi_\alpha \pi_\beta \rangle_c + \sum_\lambda t_{\alpha\lambda} \langle \varphi_\lambda \varphi_\beta \rangle_c \\ &\quad - g_B \sum_{\lambda_1 \lambda_2} \langle \alpha | \lambda_1 \lambda_2 \rangle \langle \bar{\psi}_{i\lambda_1} \psi_{i\lambda_2} \varphi_\beta \rangle_c, \end{aligned} \quad (38)$$

$$\begin{aligned} \partial_t \langle \pi_\alpha \pi_\beta \rangle_c &= \sum_\lambda t_{\alpha\lambda} \langle \varphi_\lambda \pi_\beta \rangle_c + t_{\beta\lambda} \langle \pi_\alpha \varphi_\lambda \rangle_c \\ &\quad - g_B \sum_{\lambda_1 \lambda_2} \langle \alpha | \lambda_1 \lambda_2 \rangle \langle \bar{\psi}_{i\lambda_1} \psi_{i\lambda_2} \pi_\beta \rangle_c \\ &\quad - g_B \sum_{\lambda_1 \lambda_2} \langle \beta | \lambda_1 \lambda_2 \rangle \langle \bar{\psi}_{i\lambda_1} \psi_{i\lambda_2} \pi_\alpha \rangle_c, \end{aligned} \quad (39)$$

$$\begin{aligned} \partial_t \langle \bar{\psi}_{a\alpha} \psi_{b\beta} \rangle_c &= \sum_\lambda \tilde{t}_{\lambda\alpha}^{la} \langle \bar{\psi}_{l\lambda} \psi_{b\beta} \rangle_c - \tilde{t}_{\beta\lambda}^{bn} \langle \bar{\psi}_{a\alpha} \psi_{n\lambda} \rangle_c \\ &\quad + i g_B \beta_{la} \sum_{\lambda_1 \lambda_2} \langle \alpha | \lambda_1 \lambda_2 \rangle \langle \bar{\psi}_{l\lambda_1} \psi_{b\beta} \varphi_{\lambda_2} \rangle_c \\ &\quad - i g_B \beta_{bl} \sum_{\lambda_1 \lambda_2} \langle \beta | \lambda_1 \lambda_2 \rangle \langle \bar{\psi}_{a\alpha} \psi_{l\lambda_1} \varphi_{\lambda_2} \rangle_c, \end{aligned} \quad (40)$$

Due to their length the equations of motion for further Green functions are shifted to Appendix B. A diagrammatical representation particularly for the time evolution of a mixed 3-point function is given in Appendix C.

By using a finite basis of plane waves two cutoffs – ultraviolet as well as infrared – are introduced. For a given boxsize L the difference between two neighboring momenta is $\Delta k = 2\pi/L$ such that a basis of n states in $1 + 1$ dimensions contains an ultraviolet momentum-cutoff of $k_{cut} = (n - 1)\Delta k/2$.

2.2 The renormalization scheme for Yukawa-theory

Before carrying out any calculations on the basis of the correlation dynamical equations of motion one first has to renormalize the Yukawa-theory. In $1 + 1$ dimensions the theory contains two divergent 1PI-diagrams, the tadpole diagram and the polarization diagram (cf. Fig. 1), as can be seen directly by evaluating the superficial degree of divergence.

The tadpole diagram – due to its structure with only one external boson line – requires a renormalization of the external boson source. Therefore we have to consider a Yukawa-Lagrangian extended by an additional boson source term $J_B \Phi$. The renormalization is then done by introducing a source counterterm which cancels exactly the divergences arising from the tadpole diagram. In contrast to this prescription the bare source J_B is fixed in the GEP approach by the requirement that the energy density has to have a extremum at $\Phi_0 = 0$ (cf. [14]). The resulting difference between the unrenormalized and the renormalized source in GEP calculation is fully equivalent to the counterterm of the diagrammatical source renormalization. One has to keep in mind that this renormalization procedure for the boson source does not affect the correlation dynamical equations of motion of the connected equal-time Green functions. This results from the fact that the boson source term only appears in the equations of motion for the 1-point functions. Since the 1-point functions are taken to be fixed by means of the separation (16) no adjustments in the integration procedure are necessary.

The handling of the divergent polarization diagram, however, is more sophisticated. It turns out that the only possibility to get rid of the divergence consists in a multiplicative renormalization of the coupling constant. In the continuum the renormalized coupling constant has to be defined as

$$g_R^2 = g_B^2 I_0(M), \quad (41)$$

where I_0 is an – in $1+1$ dimensions logarithmically divergent – integral of the type

$$I_n(\hat{m}) = \int \frac{dk}{2\pi} \hat{\omega}_k^{2n-1}(\hat{m}), \quad \hat{\omega}_k(\hat{m}) = \sqrt{\vec{k}^2 + \hat{m}^2}. \quad (42)$$

Thus for a finite renormalized coupling constant the bare coupling has to be infinitesimally small. We adopt the renormalization scheme of Ref. [14].

It is worth mentioning that there is no other renormalization prescription possible. A mass renormalization, which is the naive approach to a diagram of that structure, is not viable due to the equivalence of the renormalized masses and the effective masses at $\Phi_0 = 0$ in the GEP-formulation. As a consequence the renormalized and unrenormalized masses are the same for the bosons as well as for the fermions, respectively. On the other hand, a renormalization of the wavefunctions does also not lead to a solution since the effective potential will become unbounded from below.

The GEP-calculation in the continuum leads to the following approximation for the effective potential of the Yukawa-theory in 1 + 1 dimensions:

$$V_{GEP}^{cont}(\Phi_0) = \left[\frac{1}{2}m^2 - g_R^2 \right] \Phi_0^2 . \quad (43)$$

In order to compare the GEP solution with a correlation dynamical calculation one has to modify this expression due to the evaluation of the theory in discretized momentum space. In this case we remain with the following expression for a discretized GEP:

$$V_{GEP}^{dis}(\Phi_0) = 2 S_1(M) - 2 S_1(M + g_B \Phi_0) + 2Mg_B \Phi_0 S_0(M) + \frac{1}{2}m^2 \Phi_0^2 . \quad (44)$$

In comparison to the continuum GEP the integrals are replaced by the corresponding sums:

$$S_n(\hat{m}) = \frac{1}{L} \sum_i \hat{\omega}_{k_i}^{2n-1}(\hat{m}) , \quad \hat{\omega}_{k_i}(\hat{m}) = \sqrt{\vec{k}_i^2 + \hat{m}^2} . \quad (45)$$

We note that in the GEP as well as in any correlation dynamical calculation the vacuum expectation values with respect to the perturbative vacuum are subtracted. Finally, the multiplicative renormalization procedure for the Yukawa coupling constant has to be modified in the same way:

$$g_R^2 = g_B^2 S_0(M) . \quad (46)$$

3 Numerical results

3.1 2- and 3-point approximations

We first investigate the structure of the effective potential of the Yukawa theory in $1 + 1$ dimensions in the lowest orders of correlation dynamics, i.e. in 2-point and 3-point approximation. In these calculations the effective potential is generated via an adiabatic switching of the coupling constant g_R in time. The coupling constant is increased linearly – starting from the unperturbed groundstate with $g_R = 0$ – according to $g_R/m = \alpha t$, where t denotes the propagation time and α the “adiabaticity” parameter. In the limit $\alpha \rightarrow 0$ the Gell-Mann and Low theorem guarantees that the groundstate of the correlated system for fixed coupling g_R is reached [16]. For a detailed discussion of the applicability of this method we refer to Ref. [13], where this has been investigated explicitly for Φ^4 -theory. In the present case we only show that the applicability is given for all couplings in the correlation dynamical 2-point approximation. For the calculations we use $m = M = 5$ MeV while the system of equations is integrated in a basis of 19 plane waves and a boxsize $L = 100$ fm.

To show the adiabatic convergence we display the real part of one coefficient of the connected Green function $\langle \bar{\psi}_1 \psi_2 \rangle_c$ in $Y_{1+1}CD(2)$ -approximation evaluated for various parameters α from $\alpha = 10^{-1}$ c/fm to $\alpha = 2000^{-1}$ c/fm for a bosonic field expectation value $\Phi_0 = 0$ (cf. Fig. 2). With decreasing α one finds a reduction of the oscillation amplitudes. The corresponding increase of the oscillation frequency is a consequence of the presentation as a function of the dimensionless coupling g_R/m and therefore an artefact of the time rescaling. For $\alpha \leq 500^{-1}$ c/fm the calculations have sufficiently well converged versus an asymptotic curve. All values of the observed quantity agree very well with a corresponding discretized GEP-calculation as presented by the solid line in Fig. 2. This also holds for all other coefficients of $\langle \bar{\psi}_1 \psi_2 \rangle_c$. Furtheron – except explicitly mentioned otherwise – we use $\alpha = 2000^{-1}$ c/fm which ensures convergence in all coupling regimes investigated. In 3-point and 4-point approximation, however, this is no longer possible above some critical coupling (see below).

In Fig. 3 the effective potential of the Yukawa-theory in $1+1$ dimensions is presented in $Y_{1+1}CD(2)$ - and for comparison in discretized GEP-approximation – as a function of the dimensionless coupling constant g_R/m and the boson field expectation value Φ_0 . In both approximations one recognizes the parabolic structure of the effective potential for small renormalized coupling constants. With increasing coupling this parabola bends over and the effective potential turns negative above some critical coupling. In contrast to the pure parabolic structure of the continuum GEP (even for large g_R/m) we obtain a double-well shape in the discretized calculation. This behaviour is a direct consequence of the ultraviolet cutoff induced by the finite number of single-particle basis states and can be explained by a Taylor-expansion of the discretized effective

potential (44) around $\Phi_0 = 0$,

$$\begin{aligned}
V_{GEP}^{dis}(\Phi_0) &= \left[\frac{1}{2}m^2 - g_R^2 + g_B^2 M^2 S_{-1}(M) \right] \Phi_0^2 \\
&+ g_B^3 \Phi_0^3 \left[M S_{-1}(M) - M^3 S_{-2}(M) \right] \\
&+ g_B^4 \Phi_0^4 \left[\frac{1}{4} S_{-1}(M) - \frac{3}{2} M^2 S_{-2}(M) + \frac{5}{4} M^4 S_{-3}(M) \right] + O(\Phi_0^5).
\end{aligned} \tag{47}$$

Due to the ultraviolet cutoff the bare coupling constant does not become infinitesimally small but assumes a finite value. Therefore, in addition to the terms in the continuum-limit, further contributions of higher order in Φ_0 appear. Since the coefficients of the most important terms, the S_{-1} -terms, are positive, this leads to an increase of the GEP for high values of $|\Phi_0|$.

Another feature of the correlation dynamical approximation on the 2-point-level within a finite set of basis states is the fact that for certain parameter regions the $Y_{1+1}CD(2)$ -approximation differs from the discretized GEP-calculation. However, in the continuum limit with an infinite number of basis states both approximations generate the same results since the GEP represents the stationary limit of the field-theoretical Hartree-Fock-Bogoliubov-(HFB)-approximation, which is equivalent to the correlation dynamical 2-point approximation. The difference in the discretized theory appears in all areas of the parameter plane where the effective fermion mass of the GEP-calculation $\bar{M} = M + g_B \Phi_0$ becomes negative and can be interpreted as a result of a level-crossing effect. Beyond this hyperbola in the g_R/m - Φ_0 -plane the fermion single-particle state of lowest energy in the noninteracting case, i.e. the zero momentum mode, is energetically preferred in comparison to the highest lying fermion sea-state. Usually the highest sea-state and the first particle-state in Dirac's-picture are separated by twice the effective mass of the particle. In our case, where the effective mass becomes less than zero, this leads to an interchange of these states. Since in the $Y_{1+1}CD(2)$ -approximation no pair-production in the zero momentum mode is possible within the adiabatic process, it does not reproduce the true groundstate on the 2-point-level in the parameter-regions where the level-crossing appears.

In the $Y_{1+1}CD(3)$ -approximation we find two new features in comparison to calculations on the 2-point-level. The first one is the existence of coupling regimes for small boson background fields where the propagation of the system of equations of motion breaks down. Thus results for the effective potential in $Y_{1+1}CD(3)$ -approximation are only accessible up to coupling constants of $g_R/m \approx 0.8$ for all Φ_0 . In contrast, the effective potential in 2-point approximation can be evaluated for all values of the coupling and the external background field. One finds that the correlation dynamical propagation breaks down as soon as the effective potential assumes a non-convex structure (cf. Fig. 4) for the set of parameters $(g_R/m, \Phi_0)$. This effect is known from the correlation dynamical investigations of Φ^4 -theory and was studied in Ref. [13]. The reason for the

breakdown lies in the fact that the cluster decomposition property of connected Green functions is not valid anymore in a two-phase configuration as encountered in the “non-convex” region of an effective potential, where the correct energy density has an upper bound given via a Maxwell-construction [18, 19] that can be reached dynamically as soon as the approximation scheme allows for tunneling. Due to the inadequacy of the cluster decomposition the connected Green functions are not restricted to small values, but can dominate the full Green functions. In the latter case the correlation dynamical truncation is no longer a valid approximation. It is worthwhile to point out that this unstable behaviour in the present case is not a weakness of the correlation dynamical approach since for those coupling strengths where the discretized effective potential becomes non-convex, the system is no longer bounded from below in the continuum.

The second aspect of the $Y_{1+1}CD(3)$ -approximation is the reduction of the total energy density. While the global shape of the effective potential – up to the critical coupling constant – is not changed much one finds a significant lowering of the energy density especially for boson background fields with small absolute values (cf. Fig. 5)). This effect shows its maximum influence not for $\Phi_0 = 0$, but for such combinations of the coupling constant and the external background field where the $Y_{1+1}CD(2)$ -approximation separates from the discretized GEP, i.e. where the effective fermion mass becomes zero.

The reason for this behaviour is that in the $Y_{1+1}CD(3)$ -approximation (in contrast to the $Y_{1+1}CD(2)$ -approximation) pair-production in the fermionic zero-momentum mode can take place. Thus the energy density can be lowered significantly in a region where such a state is energetically preferred. In order to understand why pair production in the fermionic zero mode is not possible in the $Y_{1+1}CD(2)$ -approximation, we treat the problem in particle-number representation. We consider the mode expansions (within a discretized momentum space) for all field operators

$$\Phi(\vec{x}) = \frac{1}{\sqrt{L}} \sum_{\alpha} \sqrt{2\omega_{\alpha}} \left[a_{\alpha} + a_{\vec{\alpha}}^{\dagger} \right] e^{i\vec{k}_{\alpha}\vec{x}}, \quad \omega_{\alpha} = \sqrt{\vec{k}_{\alpha}^2 + m^2}, \quad (48)$$

$$\Pi(\vec{x}) = \frac{-i}{\sqrt{L}} \sum_{\alpha} \sqrt{\frac{\omega_{\alpha}}{2}} \left[a_{\alpha} - a_{\vec{\alpha}}^{\dagger} \right] e^{i\vec{k}_{\alpha}\vec{x}}, \quad (49)$$

$$\Psi_i(\vec{x}) = \frac{1}{\sqrt{L}} \sum_{\alpha} \sqrt{\frac{M}{\Omega_{\alpha}}} \left[b_{\alpha} u_{i\alpha} + d_{\vec{\alpha}}^{\dagger} v_{i\vec{\alpha}} \right] e^{i\vec{k}_{\alpha}\vec{x}}, \quad \Omega_{\alpha} = \sqrt{\vec{k}_{\alpha}^2 + M^2}, \quad (50)$$

$$\bar{\Psi}_i(\vec{x}) = \frac{1}{\sqrt{L}} \sum_{\alpha} \sqrt{\frac{M}{\Omega_{\alpha}}} \left[b_{\vec{\alpha}}^{\dagger} \bar{u}_{i\vec{\alpha}} + d_{\alpha} \bar{v}_{i\alpha} \right] e^{i\vec{k}_{\alpha}\vec{x}}, \quad (51)$$

where each annihilation operator annihilates the perturbative vacuum.

Here the abbreviation $\cdot_{\vec{\alpha}}$ for the inverse momentum index is introduced according to

$$\vec{k}_{\alpha} + \vec{k}_{\vec{\alpha}} = \vec{0} \quad \forall \alpha. \quad (52)$$

Evaluating the complete equation of motion for the fermionic particle-number operator we find (using $\check{a}_\alpha = a_\alpha + a_\alpha^\dagger$):

$$\begin{aligned}
i\partial_t \langle b_\alpha^\dagger b_\alpha \rangle &= g_B M L \sum_{\lambda_1 \lambda_2} \langle 1 | \alpha \lambda_1 \lambda_2 \rangle \frac{1}{\sqrt{2 \Omega_\alpha \Omega_{\lambda_1} \omega_{\lambda_2}}} \\
&\quad \times \left\{ \langle b_\alpha^\dagger b_{\bar{\lambda}_1} \check{a}_{\bar{\lambda}_2} \rangle \bar{u}_{i\alpha} u_{i\bar{\lambda}_1} + \langle b_\alpha^\dagger d_{\bar{\lambda}_1}^\dagger \check{a}_{\bar{\lambda}_2} \rangle \bar{u}_{i\alpha} v_{i\lambda_1} \right\} \\
&\quad - g_B M L \sum_{\lambda_1 \lambda_2} \langle 1 | \alpha \lambda_1 \lambda_2 \rangle \frac{1}{\sqrt{2 \Omega_\alpha \Omega_{\lambda_1} \omega_{\lambda_2}}} \\
&\quad \times \left\{ \langle b_{\bar{\lambda}_1}^\dagger b_\alpha \check{a}_{\lambda_2} \rangle \bar{u}_{i\bar{\lambda}_1} u_{i\alpha} + \langle d_{\lambda_1} b_\alpha \check{a}_{\lambda_2} \rangle \bar{v}_{i\lambda_1} u_{i\alpha} \right\} . \tag{53}
\end{aligned}$$

In (53) only operator products with 3 creation/annihilation operators lead to a nonzero r.h.s. (even for the zero momentum mode), such that for all momenta a particle-antiparticle production is possible. In a 2-point calculation where the expectation values of the operator products are factorized, only the following terms survive,

$$\langle \bullet_\alpha \bullet_\beta \check{a}_\gamma \rangle = \langle \bullet_\alpha \bullet_\beta \rangle \langle \check{a}_\gamma \rangle = \langle \bullet_\alpha \bullet_\beta \rangle \sqrt{2 m L} \Phi_0 \delta_{\vec{k}_\gamma, \vec{0}} . \tag{54}$$

In (54) the symbols \bullet_α represent an arbitrary fermionic operator with the corresponding momentum index. In a translationally invariant system one ends up with

$$\partial_t \langle b_\alpha^\dagger b_\alpha \rangle = -2 g_B \Phi_0 \frac{k_\alpha}{\Omega_\alpha} \text{Im} \left\{ \langle b_\alpha^\dagger d_\alpha^\dagger \rangle \right\} \tag{55}$$

which becomes zero for the zero momentum mode. Thus when propagating the system in time – even with a simultaneous variation of the coupling constant – the explicit appearance of the momentum k_α in (55) prevents a change of the occupation number in the zero momentum mode.

3.2 The 4-point approximation

The highest order correlation dynamical approximation investigated in the present work is the $Y_{1+1}CD(4)$ -approximation. For these calculations we modify the size of the box to 5 fm due to the enormous increase in the number of differential equations that have to be integrated. In this approximation all connected boson 3-point functions as well as all connected 4-point functions, that contain fermion degrees of freedom, must be propagated. (Due to the special structure of the Yukawa interaction the pure bosonic connected Green functions of order 4 disappear in this approximation scheme.) For practical reasons we are limited to 11 basis states. One has to choose a smaller boxsize in order to achieve a sufficiently good ultraviolet convergence (at least for relative small boson background fields and up to coupling constants of $g_R/m = 0.8$). All other parameters, that have been used in the previous calculations, remain the same.

In $Y_{1+1}CD(4)$ -approximation we observe a novel effect for small boson background fields, i.e. the propagation becomes unstable at $\Phi_0 = 0$ already for “low” coupling constants $g_R/m < 0.4$. In the limit $\alpha \rightarrow 0$ one no longer achieves adiabatic convergence for $g_R/m \geq 0.4$ (cf. Fig. 6). These coupling strengths are much lower than those for the non-convex phase of the system. To analyse this behaviour in more detail we introduce the concept of an equal-time self energy. One way to proceed this is to define a G-matrix $G_{\alpha\beta\gamma}^{ab}$ for the connected equal-time Green functions via the following relation between the full and the unconnected parts of the mixed 3-point function:

$$\sum_{\lambda_1\lambda_2} G_{\alpha\lambda_1\lambda_2}^{la} \langle \bar{\psi}_{l\lambda_1} \psi_{b\beta} \rangle \langle \varphi_{\lambda_2} \rangle = g_B L^{3/2} \gamma_{la}^0 \sum_{\lambda_1\lambda_2} \langle \alpha|\lambda_1\lambda_2 \rangle \langle \bar{\psi}_{l\lambda_1} \psi_{b\beta} \varphi_{\lambda_2} \rangle. \quad (56)$$

Due to translational invariance only the terms with $\vec{k}_{\lambda_2} = \vec{0}$ contribute on the l.h.s. of (56) and the equation for the G-matrix reads

$$\sum_{\lambda} G_{\alpha\lambda}^{la} \langle \bar{\psi}_{l\lambda} \psi_{b\beta} \rangle = \frac{g_B L \gamma_{la}^0}{\Phi_0} \sum_{\lambda_1\lambda_2} \langle \alpha|\lambda_1\lambda_2 \rangle \langle \bar{\psi}_{l\lambda_1} \psi_{b\beta} \varphi_{\lambda_2} \rangle, \quad (57)$$

where

$$G_{\alpha\beta}^{ab} := \sum_{\gamma} G_{\alpha\beta\gamma}^{ab} \delta_{\vec{k}_{\gamma}, \vec{0}} \quad (58)$$

has been introduced. Defining the self energy by

$$\tilde{\Sigma}_{\alpha\beta}^{ab} = \frac{1}{\sqrt{L}} \sum_{\lambda} G_{\alpha\beta\lambda}^{ab} \langle \varphi_{\lambda} \rangle = \Phi_0 G_{\alpha\beta}^{ab}, \quad (59)$$

we can write the equations of motion for the fermionic 2-point function as

$$\begin{aligned} i\partial_t \langle \bar{\psi}_{a\alpha} \psi_{b\beta} \rangle &= i \sum_{\lambda} \left\{ \tilde{t}_{\lambda\alpha}^{la} \langle \bar{\psi}_{l\lambda} \psi_{b\beta} \rangle - \tilde{t}_{\beta\lambda}^{bl} \langle \bar{\psi}_{a\alpha} \psi_{l\lambda} \rangle \right\} \\ &+ \sum_{\lambda} \left\{ \tilde{\Sigma}_{\lambda\alpha}^{la} \langle \bar{\psi}_{l\lambda} \psi_{b\beta} \rangle - \tilde{\Sigma}_{\beta\lambda}^{bl} \langle \bar{\psi}_{a\alpha} \psi_{l\lambda} \rangle \right\}. \end{aligned} \quad (60)$$

The self energies contain all contributions to the time evolution that exceed the 2-point-level. Keeping this in mind one can also define the self energies directly (and omit the singularity at $\Phi_0 = 0$ in (57)), such that the interaction part in the equation of motion has the same structure as the free contribution. With regard to the observed behaviour in $Y_{1+1}CD(4)$ -approximation the self energy of the expectation value of an operator product of two fermionic particle operators is of interest:

$$\begin{aligned} i\partial_t \langle b_{\alpha}^{\dagger} b_{\beta} \rangle &= - \sum_{\lambda} \tilde{t}_{\lambda\alpha} \langle b_{\lambda}^{\dagger} b_{\beta} \rangle + \sum_{\lambda} \tilde{t}_{\beta\lambda} \langle b_{\alpha}^{\dagger} b_{\lambda} \rangle \\ &+ g_B M L \sum_{\lambda_1\lambda_2} \langle 1|\beta\lambda_1\lambda_2 \rangle \frac{1}{\sqrt{2\Omega_{\beta}\Omega_{\lambda_1}\omega_{\lambda_2}}} \end{aligned}$$

$$\begin{aligned}
& \times \left\{ \langle b_\alpha^\dagger b_{\bar{\lambda}_1} \hat{a}_{\bar{\lambda}_2} \rangle \bar{u}_{i\beta} u_{i\bar{\lambda}_1} + \langle b_\alpha^\dagger d_{\lambda_1}^\dagger \hat{a}_{\bar{\lambda}_2} \rangle \bar{u}_{i\beta} v_{i\lambda_1} \right\} \\
& - g_B M L \sum_{\lambda_1 \lambda_2} \langle 1 | \alpha \lambda_1 \lambda_2 \rangle \frac{1}{\sqrt{2 \Omega_\alpha \Omega_{\lambda_1} \omega_{\lambda_2}}} \\
& \times \left\{ \langle b_{\bar{\lambda}_1}^\dagger b_\beta \hat{a}_{\lambda_2} \rangle \bar{u}_{i\bar{\lambda}_1} u_{i\alpha} + \langle d_{\lambda_1} b_\beta \hat{a}_{\lambda_2} \rangle \bar{v}_{i\lambda_1} u_{i\alpha} \right\} . \tag{61}
\end{aligned}$$

Defining the self energy directly by

$$\begin{aligned}
\tilde{\Sigma}_{\beta\lambda} &= \frac{g_B M L}{\langle b_\alpha^\dagger b_\lambda \rangle} \sum_{\lambda_1 \lambda_2} \langle 1 | \beta \lambda_1 \lambda_2 \rangle \frac{1}{\sqrt{2 \Omega_\beta \Omega_{\lambda_1} \omega_{\lambda_2}}} \\
& \times \left\{ \langle b_\alpha^\dagger b_{\bar{\lambda}_1} \hat{a}_{\bar{\lambda}_2} \rangle \bar{u}_{i\beta} u_{i\bar{\lambda}_1} + \langle b_\alpha^\dagger d_{\lambda_1}^\dagger \hat{a}_{\bar{\lambda}_2} \rangle \bar{u}_{i\beta} v_{i\lambda_1} \right\} , \tag{62}
\end{aligned}$$

we remain with the following expression for the equation of motion (62):

$$i\partial_t \langle b_\alpha^\dagger b_\beta \rangle = - \sum_\lambda \left[\tilde{t}_{\lambda\alpha} + \tilde{\Sigma}_{\lambda\alpha} \right] \langle b_\lambda^\dagger b_\beta \rangle + \sum_\lambda \left[\tilde{t}_{\beta\lambda} + \tilde{\Sigma}_{\beta\lambda} \right] \langle b_\alpha^\dagger b_\lambda \rangle , \tag{63}$$

in which the free propagation part is given by the energy in the noninteracting case, i.e. $\tilde{t}_{\alpha\beta} = \Omega_\alpha \delta_{\alpha\beta}$. With the help of these self energies one can construct the renormalized mean-field

$$\tilde{U}_{\alpha\beta}^{ren} = (Re\tilde{\Sigma})_{\alpha\beta} \tag{64}$$

and the renormalized mean-field-hamiltonian

$$\tilde{h}_{\alpha\beta}^{ren} = \tilde{t}_{\alpha\beta} + \tilde{U}_{\alpha\beta}^{ren} . \tag{65}$$

The eigenvalues ϵ_α of (65) are the interesting quantities because they correspond to the energies of the basis states in the interacting case. Plotting the energies ϵ_α versus the dimensionless coupling constant g_R/m we obtain the following picture (Fig. 7): Whereas the single-particle energies do not change much for $g_R/m \leq 0.2$, at $g_R/m \approx 0.25$ a substantial lowering of the energy-levels – especially in the zero-momentum mode – appears. For all other momentum modes this behaviour is not so strong and shifted to higher couplings g_R/m . This contrasts the situation in the $Y_{1+1}CD(3)$ -approximation. In the correlation dynamical 3-point approximation the decrease of the single-particle energies is much slower. Here we have to mention that for this behaviour in the $Y_{1+1}CD(4)$ -calculation no – in comparison to the $Y_{1+1}CD(3)$ -approximation – additional terms appear in the self energy. Only the magnitude of the terms in the self energy (62) is changed significantly by the inclusion of the 4-point functions. Considering the occupation numbers $\langle b_\alpha^\dagger b_\alpha \rangle$ one finds – as a consequence of this rapid decrease of the single-particle energies – a very strong population of the corresponding modes for $g_R/m \approx 0.5$ in the $Y_{1+1}CD(4)$ -approximation (cf. Fig. 8). For small couplings the zero

momentum mode is occupied only weakly while the occupation number has its maximum in the first mode; all other modes follow corresponding to their single-particle energies. When reaching the critical coupling regime the single-particle energy for the zero-momentum mode drops substantially such that it can be populated to a high degree. Finally, for increasing g_R/m the occupation number of this mode exceeds those of all other momentum modes and the zero mode becomes occupied preferentially (cf. Fig. 9). Here we also find a different picture in the $Y_{1+1}CD(3)$ -approximation, where the lowest momentum modes are populated only for very high coupling constants and with much less intensity (cf. Fig. 8).

The same behaviour can be seen in the alternative representation in Fig. 10 (upper part), where the occupation numbers of the modes as well as the dimensionless coupling constant are displayed logarithmically. For small coupling constants the occupation numbers of all momentum modes are almost the same in both approximations. The linear increase indicates a scaling of the occupation numbers with approximately the square of the (unrenormalized) coupling constant. We recall that, with exception of the zero-momentum mode, the occupation numbers of all other modes in $Y_{1+1}CD(3)$ -approximation agree quite well with those of the 2-point calculations. One can recover this dependence on g_R/m analytically from the GEP-solution in the small coupling limit. Furthermore, one finds a scaling of the occupation numbers with Φ_0^2 if the absolute value of Φ_0 is small. Thus for low g_R/m the occupation numbers of all momentum modes (except the zero mode) are mainly determined by the 2-point contributions. The particle number in the zeroth mode is only influenced – due to the missing property of pair-production in the 2-point approximation – by contributions of higher order connected Green functions. Consequently the zero mode (although preferred by energy) is less populated than all residual modes. Its relative occupation number is increased in the $Y_{1+1}CD(3)$ -approximation for growing coupling g_R/m . In $Y_{1+1}CD(4)$ -approximation we find approximately the same particle number (compared to the $Y_{1+1}CD(3)$ -approximation) for small g_R/m . For coupling constants $g_R/m \approx 0.2$ the influence of the 4-point contribution begins to grow and first leads to an increase of the occupation number of the zero mode, then of all other modes with growing g_R/m .

We have to point out that the observed effect persists in the ultraviolet limit and is not an effect of the regularization. This we conclude from the fact that the decrease of the single-particle energies and the subsequent increase of the occupation numbers appears in all momentum modes. We speculate that this new effect is due to condensation of fermion-antifermion pairs that only appears on the 4-point-level.

In order to demonstrate that the step rise in the occupation number of the zero momentum mode is not an artefact of the lower boxsize L we show in Fig. 10 (lower part) the occupation number of the lowest momentum mode as a function of g_R/m for three boxsizes ($L = 5$ fm, 20 fm, 100 fm) in 3-point approximation using the usual parameterset of the 4-point approximation. One recognizes that for all boxsizes L the occupation number of the zero momentum mode increases only smoothly with

g_R/m and no breakdown appears in the displayed coupling regime. Without explicit representation we note that the occupation numbers for all higher lying modes in the 3-point approximation essentially show a straight line as in the upper part of Fig. 10, however, shifted as a function of L . Therefore the difference between the $Y_{1+1}CD(4)$ - and the $Y_{1+1}CD(3)$ -approximation is substantial and not just an effect of the different L chosen in both approximations before.

The regime of the classical boson field Φ_0 , where this behaviour can be found, is very small. Even for $|\Phi_0| \approx 1.0$ higher quantum correlations are suppressed so that the effect is no longer present. To illustrate the dependence on Φ_0 we show in Fig. 11 the correlation strength of the mixed 4-point-function $\langle \bar{\Psi}\Psi\Pi\Pi \rangle$, i.e. the quantity

$$\left| \frac{\langle \bar{\Psi}\Psi\Pi\Pi \rangle_c}{\langle \bar{\Psi}\Psi\Pi\Pi \rangle} \right|, \quad (66)$$

(which plays an important role for the applicability of the correlation dynamical approach [13]) as a function of g_R/m for various Φ_0 . While the correlation strength increases smoothly for small couplings, it grows rapidly for a Φ_0 dependent – critical coupling. Sharply peaked minima are a result of a change in sign in (66). As discussed in detail in [13] a high correlation strength is always connected with an increasing instability of the propagation which in the present case leads to a breakdown. Here we find that the stability of the system depends strongly on the absolute value of Φ_0 ; for $\Phi_0 = 0.0$ the effect is observed first and is followed by Φ_0 -values of ± 0.1 and ± 0.2 , respectively. For boson background fields $\Phi_0 \approx 1$ the system becomes unstable only for relatively strong couplings $g_R/m \approx 1.5$, which is in the regime of critical coupling constants as observed in the 3-point approximation. Thus the discussed effect in the 4-point approximation is limited to small background fields where quantum fluctuations are most prominent.

4 Summary

In the present work we have investigated the groundstate properties of the Yukawa-theory in $1 + 1$ dimensions using the method of correlation dynamics. We derived the infinite coupled hierarchy of equations of motion for connected equal-time Green functions and introduced three different truncation schemes, i.e. the 2-point-, 3-point- and 4-point approximation. Furtheron, we discussed the necessary renormalization prescription for the Yukawa-theory in $1 + 1$ dimensions which – besides an implicit counterterm renormalization of the boson source – consists in a multiplicative renormalization of the coupling constant.

In our numerical calculations we found the following results:

- The generation of a correlated eigenstate of the interacting theory is possible by adiabatically switching-on the coupling constant (in line with the Gell-Mann and Low theorem).

- The effective potentials in $Y_{1+1}CD(2)$ - and discretized GEP-approximation differ in the regime of “negative effective fermion masses” in case of a finite basis set due to an infrared- and ultraviolet-cutoff. These differences vanish in the infrared as well as in the ultraviolet limit and are due to the noninclusion of zero mode pair production in $Y_{1+1}CD(2)$ -approximation.
- In the $Y_{1+1}CD(3)$ -approximation the propagation breaks down in the non-convex region of the effective potential where the continuum theory becomes unbounded from below; this is also known from the correlation dynamical investigations of Φ^4 -theory and can be attributed to tunneling [13].
- In the $Y_{1+1}CD(4)$ -approximation a novel effect is observed, which has no analogon in the pure bosonic theories investigated so far. Here the propagation breaks down already for small couplings g_R/m , which is no longer a consequence of the transition to the non-convex parameter regime, but due to strong correlations induced by higher order connected Green functions in the fermionic sector. The associated lowering of the single-particle energies leads to a strong population of the previously weakly occupied zero momentum mode and finally to an increasing instability of the system. We speculate that this new effect is due to a condensation of fermion-antifermion pairs, but cannot prove this explicitly due to the limited set of basis states that can be employed numerically.

The last effect, that persists in the ultraviolet limit, shows that novel phenomena appear in a theory with fermionic degrees of freedom since such a behaviour was not observed in any pure boson theory so far. Furthermore, it demonstrates the importance of quantum correlations of higher order especially for low or vanishing background fields Φ_0 . It remains to be seen if such effects will persist also in gauge field theories such as QCD where the correlation dynamical approach has been formulated in [20].

B Hierarchy of equations of motion for connected equal-time Green functions in a single-particle basis

$$\partial_t \langle \varphi_\alpha \varphi_\beta \varphi_\gamma \rangle_c = \langle \pi_\alpha \varphi_\beta \varphi_\gamma \rangle_c + \langle \varphi_\alpha \pi_\beta \varphi_\gamma \rangle_c + \langle \varphi_\alpha \varphi_\beta \pi_\gamma \rangle_c \quad (70)$$

$$\begin{aligned} \partial_t \langle \pi_\alpha \varphi_\beta \varphi_\gamma \rangle_c &= \langle \pi_\alpha \pi_\beta \varphi_\gamma \rangle_c + \langle \pi_\alpha \varphi_\beta \pi_\gamma \rangle_c + \sum_\lambda t_{\alpha\lambda} \langle \varphi_\lambda \varphi_\beta \varphi_\gamma \rangle_c \\ &\quad - g_B \sum_{\lambda_1 \lambda_2} \langle \alpha | \lambda_1 \lambda_2 \rangle \langle \bar{\psi}_{i\lambda_1} \psi_{i\lambda_2} \varphi_\beta \varphi_\gamma \rangle_c \end{aligned} \quad (71)$$

$$\begin{aligned} \partial_t \langle \pi_\alpha \pi_\beta \varphi_\gamma \rangle_c &= \langle \pi_\alpha \pi_\beta \pi_\gamma \rangle_c + \sum_\lambda t_{\alpha\lambda} \langle \varphi_\lambda \pi_\beta \varphi_\gamma \rangle_c + t_{\beta\lambda} \langle \pi_\alpha \varphi_\lambda \varphi_\gamma \rangle_c \\ &\quad - g_B \sum_{\lambda_1 \lambda_2} \langle \alpha | \lambda_1 \lambda_2 \rangle \langle \bar{\psi}_{i\lambda_1} \psi_{i\lambda_2} \pi_\beta \varphi_\gamma \rangle_c \\ &\quad - g_B \sum_{\lambda_1 \lambda_2} \langle \beta | \lambda_1 \lambda_2 \rangle \langle \bar{\psi}_{i\lambda_1} \psi_{i\lambda_2} \pi_\alpha \varphi_\gamma \rangle_c \end{aligned} \quad (72)$$

$$\begin{aligned} \partial_t \langle \pi_\alpha \pi_\beta \pi_\gamma \rangle_c &= \sum_\lambda t_{\alpha\lambda} \langle \varphi_\lambda \pi_\beta \pi_\gamma \rangle_c + t_{\beta\lambda} \langle \pi_\alpha \varphi_\lambda \pi_\gamma \rangle_c + t_{\gamma\lambda} \langle \pi_\alpha \pi_\lambda \varphi_\gamma \rangle_c \\ &\quad - g_B \sum_{\lambda_1 \lambda_2} \langle \alpha | \lambda_1 \lambda_2 \rangle \langle \bar{\psi}_{i\lambda_1} \psi_{i\lambda_2} \pi_\beta \pi_\gamma \rangle_c \\ &\quad - g_B \sum_{\lambda_1 \lambda_2} \langle \beta | \lambda_1 \lambda_2 \rangle \langle \bar{\psi}_{i\lambda_1} \psi_{i\lambda_2} \pi_\alpha \pi_\gamma \rangle_c \\ &\quad - g_B \sum_{\lambda_1 \lambda_2} \langle \gamma | \lambda_1 \lambda_2 \rangle \langle \bar{\psi}_{i\lambda_1} \psi_{i\lambda_2} \pi_\alpha \pi_\beta \rangle_c \end{aligned} \quad (73)$$

$$\begin{aligned} \partial_t \langle \bar{\psi}_{a\alpha} \psi_{b\beta} \varphi_\gamma \rangle_c &= \sum_\lambda \tilde{t}_{\lambda\alpha}^{la} \langle \bar{\psi}_{l\lambda} \psi_{b\beta} \varphi_\gamma \rangle_c - \tilde{t}_{\beta\lambda}^{bl} \langle \bar{\psi}_{a\alpha} \psi_{l\lambda} \varphi_\gamma \rangle_c \\ &\quad + ig_B \beta_{la} \sum_{\lambda_1 \lambda_2} \langle \alpha | \lambda_1 \lambda_2 \rangle \langle \bar{\psi}_{l\lambda_1} \psi_{b\beta} \varphi_{\lambda_2} \varphi_\gamma \rangle_c \\ &\quad - ig_B \beta_{bl} \sum_{\lambda_1 \lambda_2} \langle \beta | \lambda_1 \lambda_2 \rangle \langle \bar{\psi}_{a\alpha} \psi_{l\lambda_1} \varphi_{\lambda_2} \varphi_\gamma \rangle_c \\ &\quad + ig_B \beta_{la} \sum_{\lambda_1 \lambda_2} \langle \alpha | \lambda_1 \lambda_2 \rangle \langle \bar{\psi}_{l\lambda_1} \psi_{b\beta} \rangle_c \langle \varphi_{\lambda_2} \varphi_\gamma \rangle_c \\ &\quad - ig_B \beta_{bl} \sum_{\lambda_1 \lambda_2} \langle \beta | \lambda_1 \lambda_2 \rangle \langle \bar{\psi}_{a\alpha} \psi_{l\lambda_1} \rangle_c \langle \varphi_{\lambda_2} \varphi_\gamma \rangle_c \\ &\quad + \langle \bar{\psi}_{a\alpha} \psi_{b\beta} \pi_\gamma \rangle_c \end{aligned} \quad (74)$$

$$\begin{aligned}
\partial_t \langle \bar{\psi}_{a\alpha} \psi_{b\beta} \pi_\gamma \rangle_c &= \sum_\lambda \tilde{t}_{\lambda\alpha}^{la} \langle \bar{\psi}_{l\lambda} \psi_{b\beta} \pi_\gamma \rangle_c - \tilde{t}_{\beta\lambda}^{bl} \langle \bar{\psi}_{a\alpha} \psi_{l\lambda} \pi_\gamma \rangle_c \\
&+ \sum_\lambda t_{\gamma\lambda} \langle \bar{\psi}_{a\alpha} \psi_{b\beta} \varphi_\lambda \rangle_c \\
&+ ig_B \beta_{la} \sum_{\lambda_1 \lambda_2} \langle \alpha | \lambda_1 \lambda_2 \rangle \langle \bar{\psi}_{l\lambda_1} \psi_{b\beta} \varphi_{\lambda_2} \pi_\gamma \rangle_c \\
&- ig_B \beta_{bl} \sum_{\lambda_1 \lambda_2} \langle \beta | \lambda_1 \lambda_2 \rangle \langle \bar{\psi}_{a\alpha} \psi_{l\lambda_1} \varphi_{\lambda_2} \pi_\gamma \rangle_c \\
&+ ig_B \beta_{la} \sum_{\lambda_1 \lambda_2} \langle \alpha | \lambda_1 \lambda_2 \rangle \langle \bar{\psi}_{l\lambda_1} \psi_{b\beta} \rangle_c \langle \varphi_{\lambda_2} \pi_\gamma \rangle_c \\
&- ig_B \beta_{bl} \sum_{\lambda_1 \lambda_2} \langle \beta | \lambda_1 \lambda_2 \rangle \langle \bar{\psi}_{a\alpha} \psi_{l\lambda_1} \rangle_c \langle \varphi_{\lambda_2} \pi_\gamma \rangle_c \\
&- g_B \sum_{\lambda_1 \lambda_2} \langle \gamma | \lambda_1 \lambda_2 \rangle \langle \bar{\psi}_{a\alpha} \psi_{b\beta} \bar{\psi}_{i\lambda_1} \psi_{i\lambda_2} \rangle_c \\
&- g_B \sum_{\lambda_1 \lambda_2} \langle \gamma | \lambda_1 \lambda_2 \rangle \langle \bar{\psi}_{a\alpha} \psi_{i\lambda_2} \rangle_c \langle \bar{\psi}_{i\lambda_1} \psi_{b\beta} \rangle_c
\end{aligned} \tag{75}$$

$$\begin{aligned}
\partial_t \langle \bar{\psi}_{a\alpha} \psi_{b\beta} \varphi_\gamma \varphi_\delta \rangle_c &= \sum_\lambda \tilde{t}_{\lambda\alpha}^{la} \langle \bar{\psi}_{l\lambda} \psi_{b\beta} \varphi_\gamma \varphi_\delta \rangle_c - \tilde{t}_{\beta\lambda}^{bl} \langle \bar{\psi}_{a\alpha} \psi_{l\lambda} \varphi_\gamma \varphi_\delta \rangle_c \\
&+ ig_B \beta_{la} \sum_{\lambda_1 \lambda_2} \langle \alpha | \lambda_1 \lambda_2 \rangle \langle \bar{\psi}_{l\lambda_1} \psi_{b\beta} \varphi_{\lambda_2} \varphi_\gamma \varphi_\delta \rangle_c \\
&+ ig_B \beta_{la} \sum_{\lambda_1 \lambda_2} \langle \alpha | \lambda_1 \lambda_2 \rangle \langle \bar{\psi}_{l\lambda_1} \psi_{b\beta} \varphi_\gamma \rangle_c \langle \varphi_{\lambda_2} \varphi_\delta \rangle_c \\
&+ ig_B \beta_{la} \sum_{\lambda_1 \lambda_2} \langle \alpha | \lambda_1 \lambda_2 \rangle \langle \bar{\psi}_{l\lambda_1} \psi_{b\beta} \varphi_\delta \rangle_c \langle \varphi_{\lambda_2} \varphi_\gamma \rangle_c \\
&- ig_B \beta_{bl} \sum_{\lambda_1 \lambda_2} \langle \beta | \lambda_1 \lambda_2 \rangle \langle \bar{\psi}_{a\alpha} \psi_{l\lambda_1} \varphi_{\lambda_2} \varphi_\gamma \varphi_\delta \rangle_c \\
&- ig_B \beta_{bl} \sum_{\lambda_1 \lambda_2} \langle \beta | \lambda_1 \lambda_2 \rangle \langle \bar{\psi}_{a\alpha} \psi_{l\lambda_1} \varphi_\gamma \rangle_c \langle \varphi_{\lambda_2} \varphi_\delta \rangle_c \\
&- ig_B \beta_{bl} \sum_{\lambda_1 \lambda_2} \langle \beta | \lambda_1 \lambda_2 \rangle \langle \bar{\psi}_{a\alpha} \psi_{l\lambda_1} \varphi_\delta \rangle_c \langle \varphi_{\lambda_2} \varphi_\gamma \rangle_c \\
&+ \langle \bar{\psi}_{a\alpha} \psi_{b\beta} \pi_\gamma \varphi_\delta \rangle_c + \langle \bar{\psi}_{a\alpha} \psi_{b\beta} \varphi_\gamma \pi_\delta \rangle_c
\end{aligned} \tag{76}$$

$$\begin{aligned}
\partial_t \langle \bar{\psi}_{a\alpha} \psi_{b\beta} \pi_\gamma \varphi_\delta \rangle_c &= \sum_\lambda \tilde{t}_{\lambda\alpha}^{la} \langle \bar{\psi}_{l\lambda} \psi_{b\beta} \pi_\gamma \varphi_\delta \rangle_c - \tilde{t}_{\beta\lambda}^{bl} \langle \bar{\psi}_{a\alpha} \psi_{l\lambda} \pi_\gamma \varphi_\delta \rangle_c \\
&+ \langle \bar{\psi}_{a\alpha} \psi_{b\beta} \pi_\lambda \pi_\delta \rangle_c + \sum_\lambda t_{\gamma\lambda} \langle \bar{\psi}_{a\alpha} \psi_{b\beta} \varphi_\lambda \varphi_\delta \rangle_c \\
&+ ig_B \beta_{la} \sum_{\lambda_1 \lambda_2} \langle \alpha | \lambda_1 \lambda_2 \rangle \langle \bar{\psi}_{l\lambda_1} \psi_{b\beta} \varphi_{\lambda_2} \pi_\gamma \varphi_\delta \rangle_c \\
&+ ig_B \beta_{la} \sum_{\lambda_1 \lambda_2} \langle \alpha | \lambda_1 \lambda_2 \rangle \langle \bar{\psi}_{l\lambda_1} \psi_{b\beta} \pi_\gamma \rangle_c \langle \varphi_{\lambda_2} \varphi_\delta \rangle_c
\end{aligned}$$

$$\begin{aligned}
& + ig_B \beta_{la} \sum_{\lambda_1 \lambda_2} \langle \alpha | \lambda_1 \lambda_2 \rangle \langle \bar{\psi}_{l\lambda_1} \psi_{b\beta} \varphi_\delta \rangle_c \langle \varphi_{\lambda_2} \pi_\gamma \rangle_c \\
& - ig_B \beta_{bl} \sum_{\lambda_1 \lambda_2} \langle \beta | \lambda_1 \lambda_2 \rangle \langle \bar{\psi}_{a\alpha} \psi_{l\lambda_1} \varphi_{\lambda_2} \pi_\gamma \varphi_\delta \rangle_c \\
& - ig_B \beta_{bl} \sum_{\lambda_1 \lambda_2} \langle \beta | \lambda_1 \lambda_2 \rangle \langle \bar{\psi}_{a\alpha} \psi_{l\lambda_1} \pi_\gamma \rangle_c \langle \varphi_{\lambda_2} \varphi_\delta \rangle_c \\
& - ig_B \beta_{bl} \sum_{\lambda_1 \lambda_2} \langle \beta | \lambda_1 \lambda_2 \rangle \langle \bar{\psi}_{a\alpha} \psi_{l\lambda_1} \varphi_\delta \rangle_c \langle \varphi_{\lambda_2} \pi_\gamma \rangle_c \\
& - g_B \sum_{\lambda_1 \lambda_2} \langle \gamma | \lambda_1 \lambda_2 \rangle \langle \bar{\psi}_{a\alpha} \psi_{i\lambda_1} \varphi_\delta \rangle_c \langle \psi_{b\beta} \bar{\psi}_{i\lambda_2} \rangle_c \\
& - g_B \sum_{\lambda_1 \lambda_2} \langle \gamma | \lambda_1 \lambda_2 \rangle \langle \bar{\psi}_{a\alpha} \psi_{i\lambda_1} \rangle_c \langle \psi_{b\beta} \bar{\psi}_{i\lambda_2} \pi_\delta \rangle_c
\end{aligned} \tag{77}$$

$$\begin{aligned}
\partial_t \langle \bar{\psi}_{a\alpha} \psi_{b\beta} \pi_\gamma \pi_\delta \rangle_c & = \sum_{\lambda} \tilde{t}_{\lambda\alpha}^{la} \langle \bar{\psi}_{l\lambda} \psi_{b\beta} \pi_\gamma \pi_\delta \rangle_c - \tilde{t}_{\beta\lambda}^{bl} \langle \bar{\psi}_{a\alpha} \psi_{l\lambda} \pi_\gamma \pi_\delta \rangle_c \\
& + \sum_{\lambda} t_{\gamma\lambda} \langle \bar{\psi}_{a\alpha} \psi_{b\beta} \varphi_\lambda \pi_\delta \rangle_c + t_{\delta\lambda} \langle \bar{\psi}_{a\alpha} \psi_{b\beta} \pi_\gamma \varphi_\lambda \rangle_c \\
& + ig_B \beta_{la} \sum_{\lambda_1 \lambda_2} \langle \alpha | \lambda_1 \lambda_2 \rangle \langle \bar{\psi}_{l\lambda_1} \psi_{b\beta} \varphi_{\lambda_2} \pi_\gamma \pi_\delta \rangle_c \\
& + ig_B \beta_{la} \sum_{\lambda_1 \lambda_2} \langle \alpha | \lambda_1 \lambda_2 \rangle \langle \bar{\psi}_{l\lambda_1} \psi_{b\beta} \pi_\gamma \rangle_c \langle \varphi_{\lambda_2} \pi_\delta \rangle_c \\
& + ig_B \beta_{la} \sum_{\lambda_1 \lambda_2} \langle \alpha | \lambda_1 \lambda_2 \rangle \langle \bar{\psi}_{l\lambda_1} \psi_{b\beta} \pi_\delta \rangle_c \langle \varphi_{\lambda_2} \pi_\gamma \rangle_c \\
& - ig_B \beta_{bl} \sum_{\lambda_1 \lambda_2} \langle \beta | \lambda_1 \lambda_2 \rangle \langle \bar{\psi}_{a\alpha} \psi_{l\lambda_1} \varphi_{\lambda_2} \pi_\gamma \pi_\delta \rangle_c \\
& - ig_B \beta_{bl} \sum_{\lambda_1 \lambda_2} \langle \beta | \lambda_1 \lambda_2 \rangle \langle \bar{\psi}_{a\alpha} \psi_{l\lambda_1} \pi_\gamma \rangle_c \langle \varphi_{\lambda_2} \pi_\delta \rangle_c \\
& - ig_B \beta_{bl} \sum_{\lambda_1 \lambda_2} \langle \beta | \lambda_1 \lambda_2 \rangle \langle \bar{\psi}_{a\alpha} \psi_{l\lambda_1} \pi_\delta \rangle_c \langle \varphi_{\lambda_2} \pi_\gamma \rangle_c \\
& - g_B \sum_{\lambda_1 \lambda_2} \langle \gamma | \lambda_1 \lambda_2 \rangle \langle \bar{\psi}_{a\alpha} \psi_{i\lambda_1} \pi_\delta \rangle_c \langle \psi_{b\beta} \bar{\psi}_{i\lambda_2} \rangle_c \\
& - g_B \sum_{\lambda_1 \lambda_2} \langle \gamma | \lambda_1 \lambda_2 \rangle \langle \bar{\psi}_{a\alpha} \psi_{i\lambda_1} \rangle_c \langle \psi_{b\beta} \bar{\psi}_{i\lambda_2} \pi_\delta \rangle_c \\
& - g_B \sum_{\lambda_1 \lambda_2} \langle \delta | \lambda_1 \lambda_2 \rangle \langle \bar{\psi}_{a\alpha} \psi_{i\lambda_1} \pi_\gamma \rangle_c \langle \psi_{b\beta} \bar{\psi}_{i\lambda_2} \rangle_c \\
& - g_B \sum_{\lambda_1 \lambda_2} \langle \delta | \lambda_1 \lambda_2 \rangle \langle \bar{\psi}_{a\alpha} \psi_{i\lambda_1} \rangle_c \langle \psi_{b\beta} \bar{\psi}_{i\lambda_2} \pi_\gamma \rangle_c
\end{aligned} \tag{78}$$

$$\begin{aligned}
\partial_t \langle \bar{\psi}_{a\alpha} \bar{\psi}_{b\beta} \psi_{c\gamma} \psi_{d\delta} \rangle_c & = \sum_{\lambda} \tilde{t}_{\lambda\alpha}^{la} \langle \bar{\psi}_{l\lambda} \bar{\psi}_{b\beta} \psi_{c\gamma} \psi_{d\delta} \rangle_c + \tilde{t}_{\lambda\alpha}^{lb} \langle \bar{\psi}_{a\alpha} \bar{\psi}_{b\lambda} \psi_{c\gamma} \psi_{d\delta} \rangle_c \\
& - \sum_{\lambda} \tilde{t}_{\gamma\lambda}^{cl} \langle \bar{\psi}_{a\alpha} \bar{\psi}_{b\beta} \psi_{l\lambda} \psi_{d\delta} \rangle_c + \tilde{t}_{\delta\lambda}^{dl} \langle \bar{\psi}_{a\alpha} \bar{\psi}_{b\beta} \psi_{c\gamma} \psi_{l\lambda} \rangle_c
\end{aligned}$$

$$\begin{aligned}
& + ig_B \beta_{la} \sum_{\lambda_1 \lambda_2} \langle \alpha | \lambda_1 \lambda_2 \rangle \langle \bar{\psi}_{l\lambda_1} \psi_{d\delta} \rangle_c \langle \bar{\psi}_{b\beta} \psi_{c\gamma} \varphi_{\lambda_2} \rangle_c \\
& - ig_B \beta_{la} \sum_{\lambda_1 \lambda_2} \langle \alpha | \lambda_1 \lambda_2 \rangle \langle \bar{\psi}_{l\lambda_1} \psi_{c\gamma} \rangle_c \langle \bar{\psi}_{b\beta} \psi_{d\delta} \varphi_{\lambda_2} \rangle_c \\
& + ig_B \beta_{lb} \sum_{\lambda_1 \lambda_2} \langle \beta | \lambda_1 \lambda_2 \rangle \langle \bar{\psi}_{l\lambda_1} \psi_{c\gamma} \rangle_c \langle \bar{\psi}_{a\alpha} \psi_{d\delta} \varphi_{\lambda_2} \rangle_c \\
& - ig_B \beta_{lb} \sum_{\lambda_1 \lambda_2} \langle \beta | \lambda_1 \lambda_2 \rangle \langle \bar{\psi}_{l\lambda_1} \psi_{d\delta} \rangle_c \langle \bar{\psi}_{a\alpha} \psi_{c\gamma} \varphi_{\lambda_2} \rangle_c \\
& + ig_B \beta_{cl} \sum_{\lambda_1 \lambda_2} \langle \gamma | \lambda_1 \lambda_2 \rangle \langle \bar{\psi}_{a\alpha} \psi_{l\lambda_1} \rangle_c \langle \bar{\psi}_{b\beta} \psi_{d\delta} \varphi_{\lambda_2} \rangle_c \\
& - ig_B \beta_{cl} \sum_{\lambda_1 \lambda_2} \langle \gamma | \lambda_1 \lambda_2 \rangle \langle \bar{\psi}_{b\beta} \psi_{l\lambda_1} \rangle_c \langle \bar{\psi}_{a\alpha} \psi_{d\delta} \varphi_{\lambda_2} \rangle_c \\
& + ig_B \beta_{dl} \sum_{\lambda_1 \lambda_2} \langle \delta | \lambda_1 \lambda_2 \rangle \langle \bar{\psi}_{b\beta} \psi_{l\lambda_1} \rangle_c \langle \bar{\psi}_{a\alpha} \psi_{c\gamma} \varphi_{\lambda_2} \rangle_c \\
& - ig_B \beta_{dl} \sum_{\lambda_1 \lambda_2} \langle \delta | \lambda_1 \lambda_2 \rangle \langle \bar{\psi}_{a\alpha} \psi_{l\lambda_1} \rangle_c \langle \bar{\psi}_{b\beta} \psi_{c\gamma} \varphi_{\lambda_2} \rangle_c
\end{aligned} \tag{79}$$

C Diagrammatical representation of the equation of motion for a connected equal-time 3-point function

To clarify the structure of the correlation dynamical equations of motion we introduce a diagrammatical representation. In Fig. 12 we demonstrate this for the equation of motion of the connected equal-time 3-point function $\langle \bar{\psi}_{a\alpha} \psi_{b\beta} \pi_\gamma \rangle_c$, where all contributions are displayed which arise from the $\bar{\Psi}$ - or the Π -part of the Green function (the contributions from field operator Ψ have the same structure as the ones from $\bar{\Psi}$ only modified by a relative minus-sign). The n-point connected equal-time Greenfunctions are represented by triangles or rectangles with a corresponding number of field operators while the greek letters at the lines – fermionic lines: solid, bosonic lines: dashed – going out of the connected Greenfunctions denote the momentum indices with respect to the chosen single-particle basis – spinor indices are neglected for transparency. We mention that all diagrams that emerge due to the application of the cluster expansion on the equation of motion for the corresponding unconnected 3-point function contribute which are connected in the usual (Feynman-)sense, while all disconnected diagrams cancel out when going over from the hierarchy for unconnected Green functions to the hierarchy for connected Green functions.

References

- [1] Stevenson, P.M.: Phys. Rev. **D32** (1985) 1389
- [2] Faber, B., Nguyen-Quang, H., Schütte, D.: Phys. Rev. **D34** (1986) 1157
- [3] Kajantie, K., Kapusta, J.: Ann. Phys. **160** (1985) 477
- [4] Bender, A., Alkofer, R.: Phys. Rev. **D53** (1996) 446
- [5] Arponen, J.: Annals of Physics **151** (1993) 311
- [6] Funke, M., Kaulfuss, U., Kümmel, H.: Phys. Rev. **D35** (1987) 621
- [7] De Blasio, F.V., Cassing, W., Tohyama, M., Bortignon, P.F., Broglia, R.A.: Phys. Rev. Lett. **68** (1992) 1663
- [8] Cassing, W., Peter, A., Pfitzner, A.: Nucl. Phys. **A561** (1993) 133
- [9] Gheregá, T., Krieg, R., Reinhard, P.G., Toepffer, C.: Nucl. Phys. **A560** (1993) 166
- [10] Häuser, J.M., Cassing, W., Peter, A.: Nucl. Phys. **A585** (1995) 727
- [11] Häuser, J.M., Cassing, W., Peter, A., Thoma, M.H.: Z. Phys. **A353** (1995) 301
- [12] Peter, A., Häuser, J.M., Thoma, M.H., Cassing, W.: Z. Phys. **C71** (1996) 515
- [13] Peter, A., Cassing, W., Häuser, J.M., Thoma, M.H.: Z. Phys. **A358** (1997) 91
- [14] Stevenson, P.M., Hajj, G.A., Reed, J.F.: Phys. Rev. **D34** (1986) 3117
- [15] Balescu, R.: *Equilibrium and Nonequilibrium Statistical Mechanics*, J. Wiley & Sons, New York 1975
- [16] Gell-Mann, M., Low, F.: Phys. Rev. **84** (1951) 350
- [17] Zinn-Justin, J.: *Quantum Field Theory and Critical Phenomena*, Clarendon Press, Oxford 1989
- [18] Peskin, M.E., Schroeder, D.V.: *Quantum Field Theory*, Addison-Wesley Publishing Company, Reading, Massachusetts 1995
- [19] Wang, S.J., Cassing, W., Häuser, J.M., Peter, A., Thoma, M.H.: Annals of Physics **242** (1995) 235

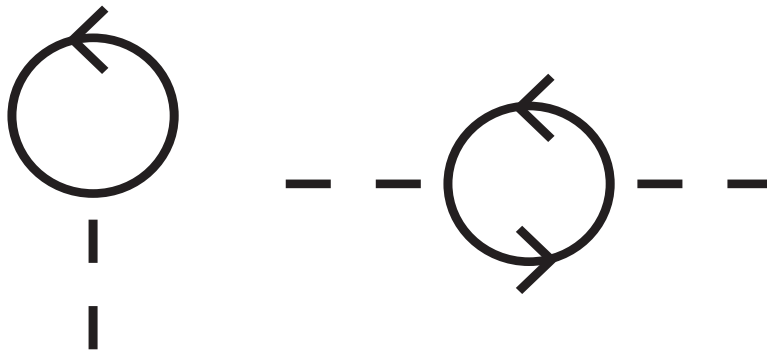


Figure 1: The divergent diagrams of Yukawa-theory in $1 + 1$ dimensions: the tadpole-diagram with superficial degree of divergence $D = 1$ (left) and the polarization-diagram with $D = 0$ (right).

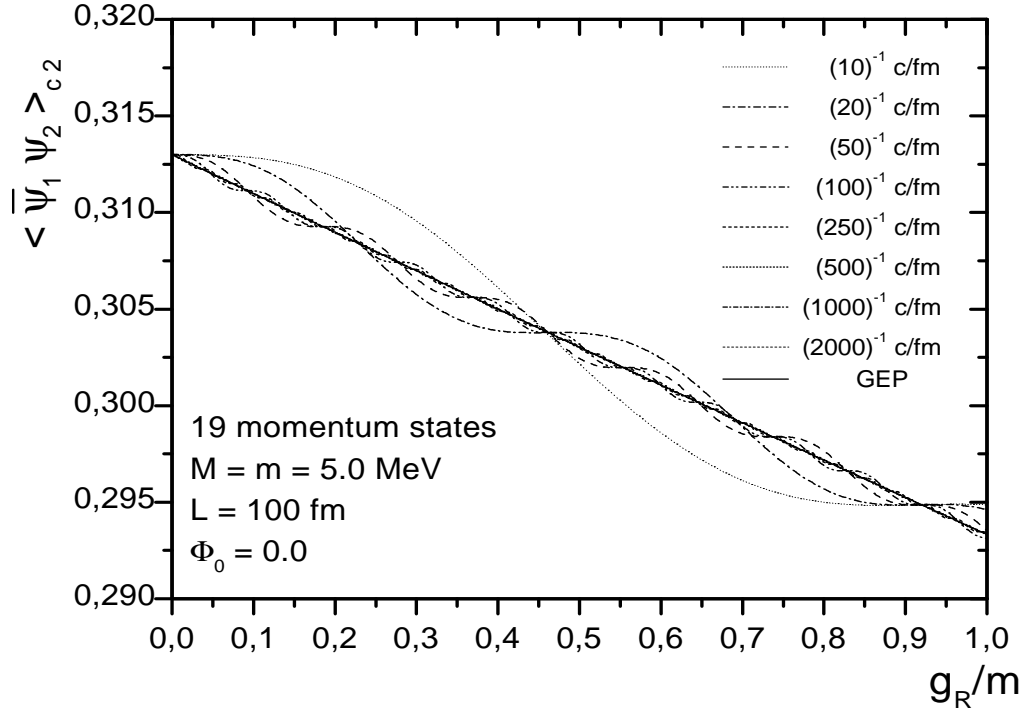


Figure 2: One coefficient of the fermionic 2-point function $\langle \bar{\psi}_1 \psi_2 \rangle_c$ as a function of the dimensionless renormalized coupling constant g_R/m for various adiabaticity parameters α . For $\alpha \rightarrow 0$ one observes convergence of the $Y_{1+1}CD(2)$ -results towards the GEP-solution (solid line).

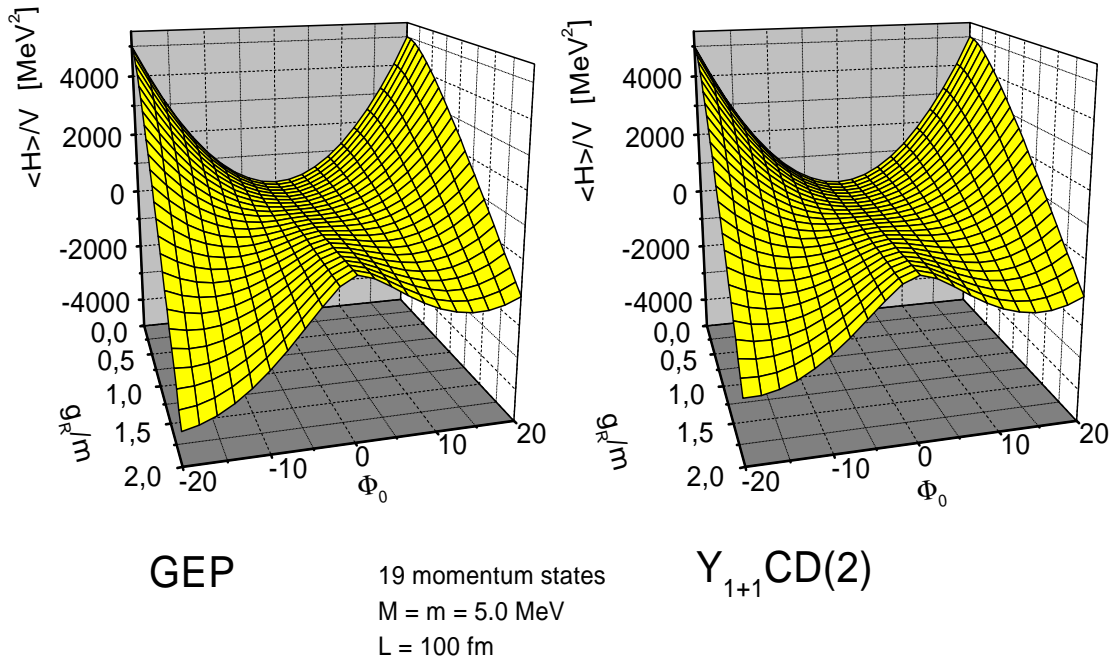


Figure 3: Effective potential in $Y_{1+1}CD(2)$ -approximation as a function of g_R/m and Φ_0 (right part) and the effective potential in the discretized GEP-approximation (left part).

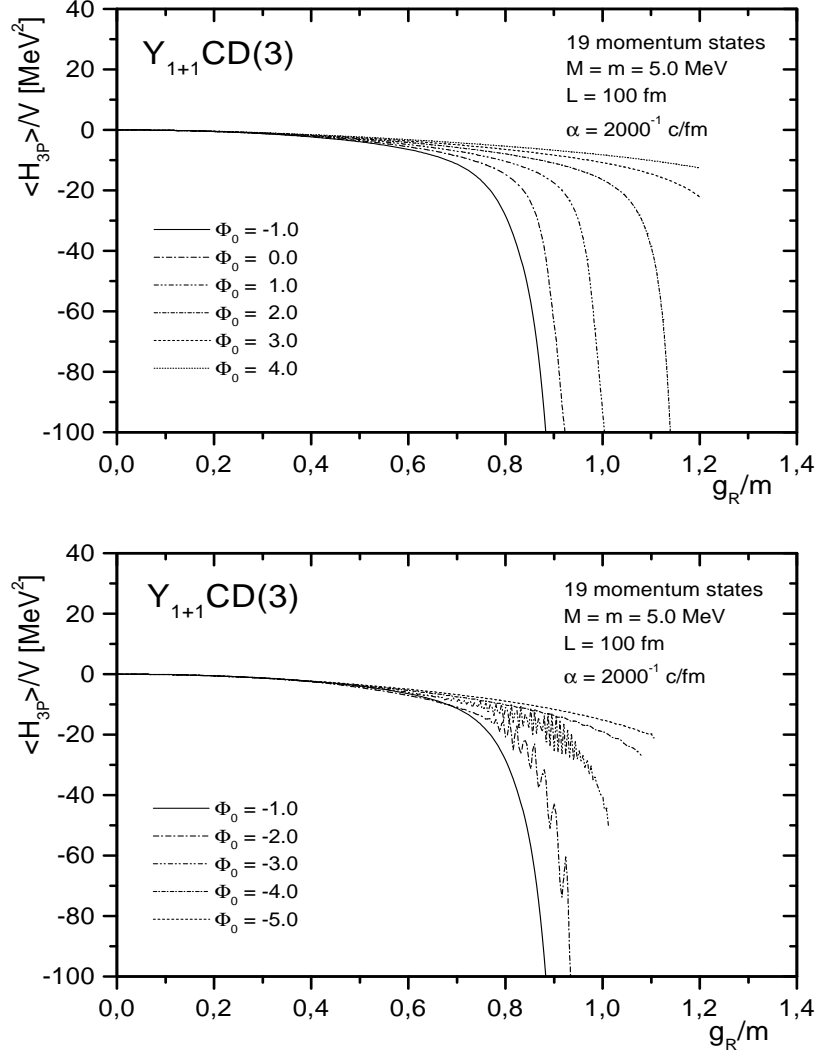


Figure 4: 3-point contribution to the total energy density for various values of the boson background field Φ_0 in $Y_{1+1}CD(3)$ -calculation; for $\Phi_0 \geq -1.0$ (upper part) and for $\Phi_0 \leq -1.0$ (lower part). The propagation breaks down for Φ_0 in the non-convex region of the effective potential. As “breakdown point” we specify those couplings at which either the propagation collapses or the energy-density of the 3-point coupling part starts to decrease rapidly.

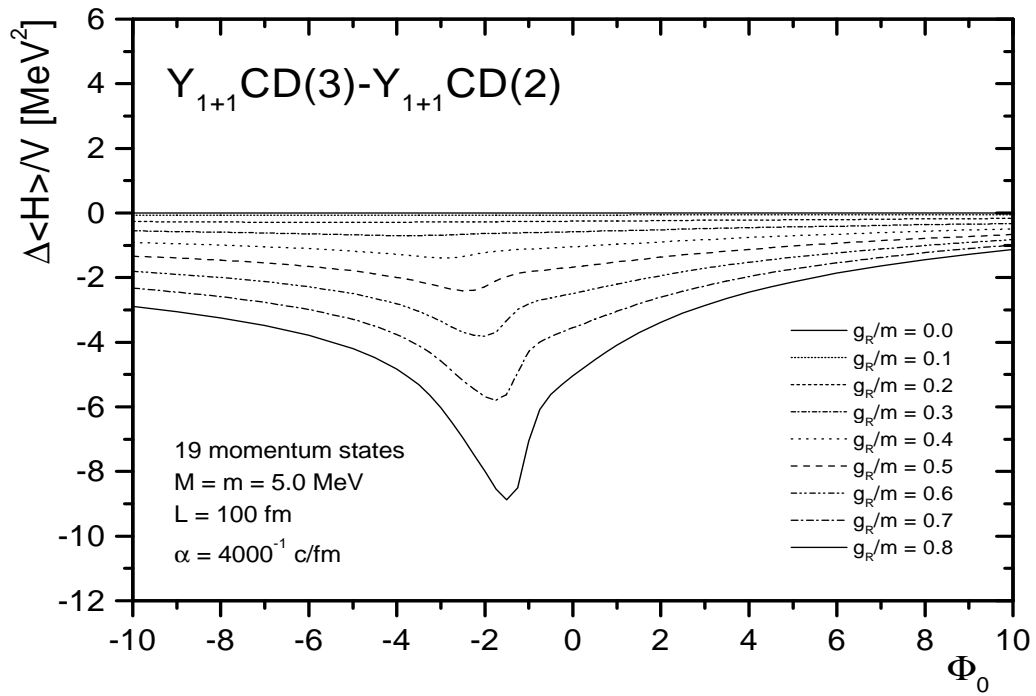


Figure 5: Difference of the effective potential in $Y_{1+1}CD(3)$ - and in $Y_{1+1}CD(2)$ -approximation.

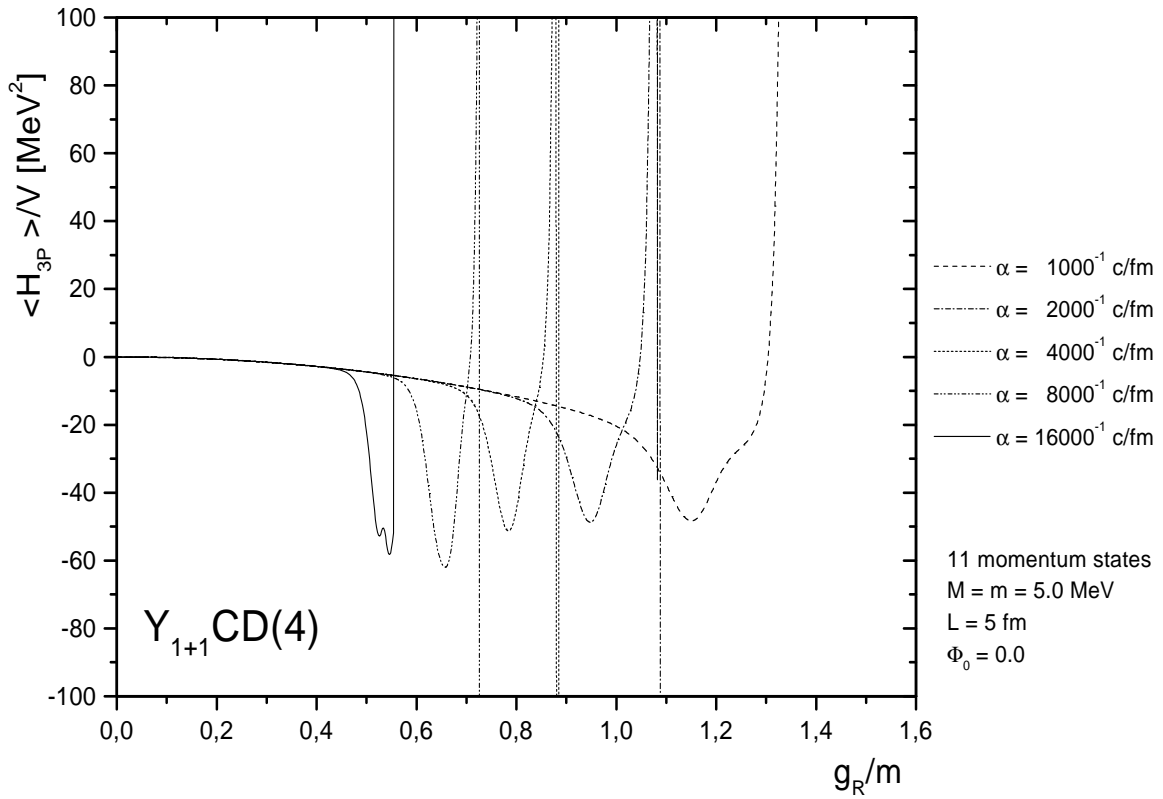


Figure 6: 3-point contribution to the energy density in $Y_{1+1}CD(4)$ -approximation for $\Phi_0 = 0$ as a function of the dimensionless coupling constant g_R/m for various adiabaticity parameters α .

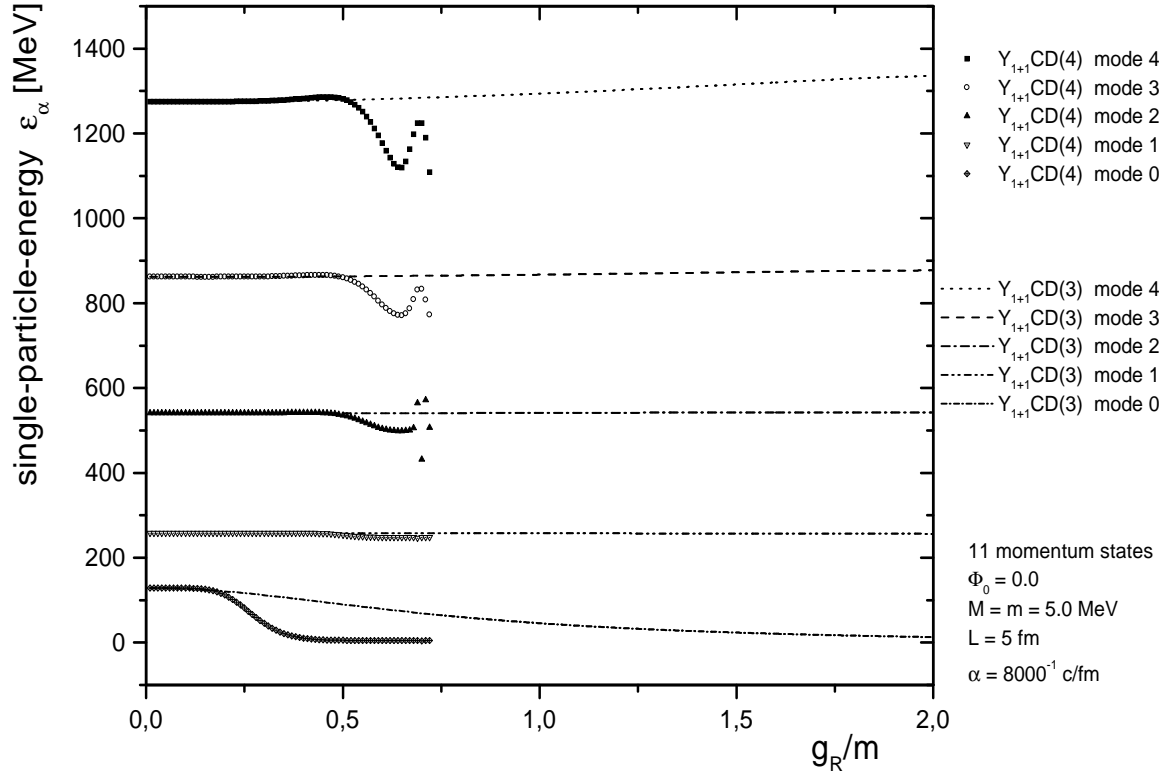


Figure 7: Single-particle energies ϵ_α for the individual fermionic momentum modes in $Y_{1+1}CD(3)$ - and $Y_{1+1}CD(4)$ -approximation as a function of the dimensionless coupling constant g_R/m . Note the massive decrease in the zeroth mode in the $Y_{1+1}CD(4)$ -calculation at $g_R/m \approx 0.25$.

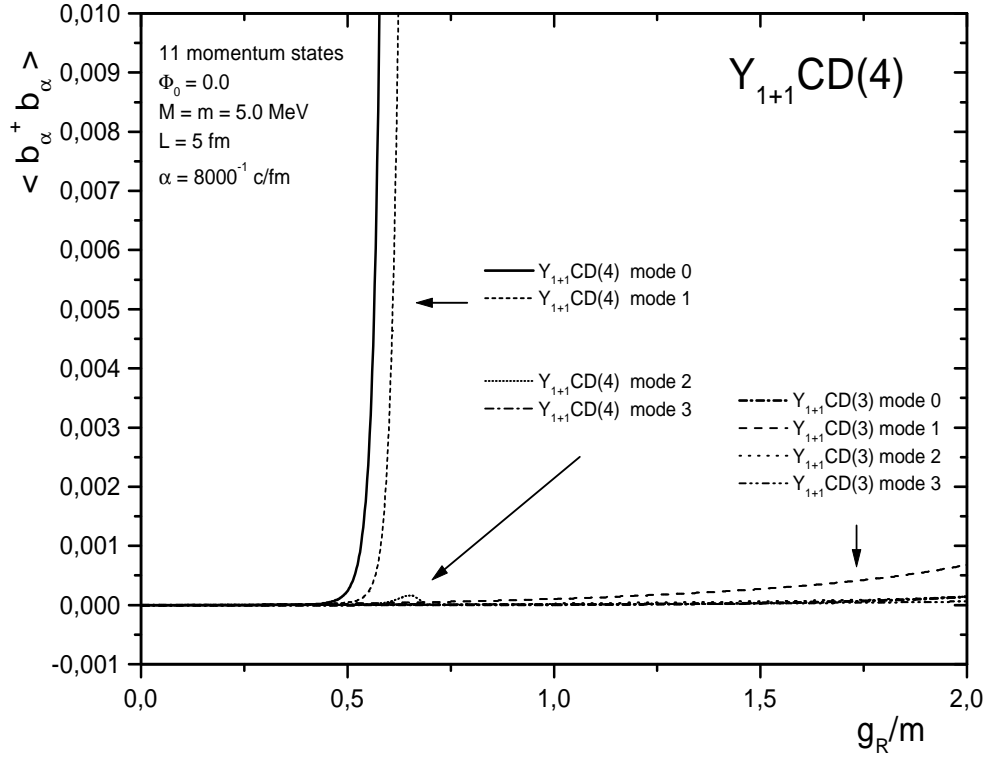
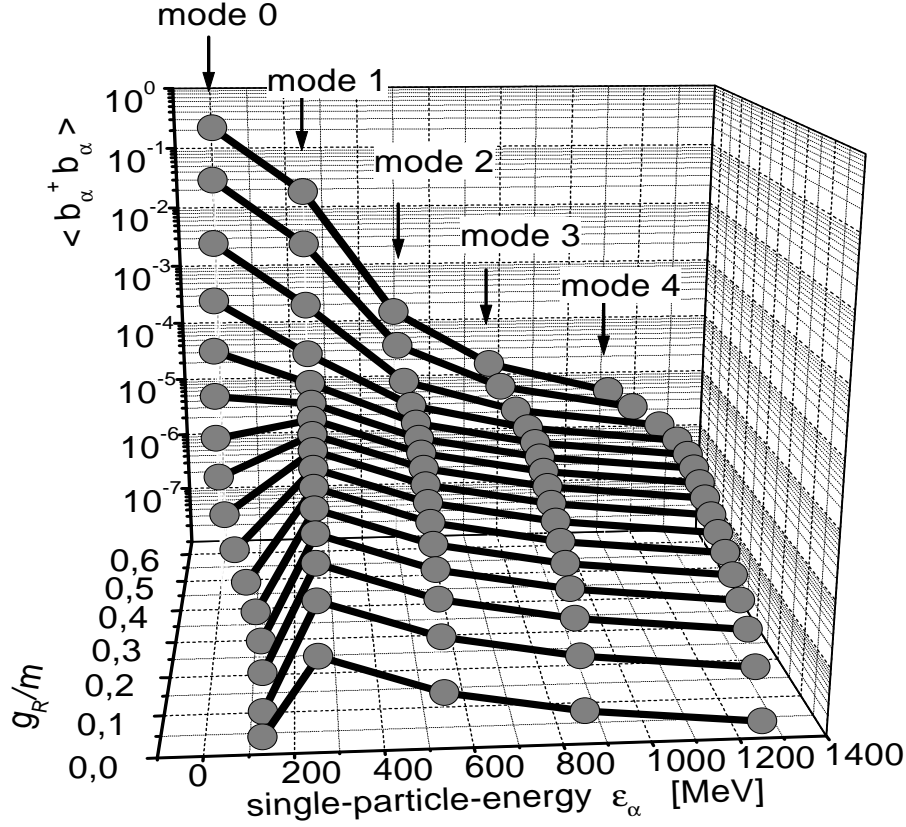


Figure 8: The occupation numbers $\langle b_\alpha^\dagger b_\alpha \rangle$ of the zeroth and first fermionic particle mode in $Y_{1+1}CD(4)$ -approximation as a function of g_R/m . In the corresponding $Y_{1+1}CD(3)$ -calculation the increase is only moderate and the occupation number of the zero-momentum mode remains small even for strong couplings.



Y_{1+1} CD(4)

11 momentum states
 $M = m = 5.0$ MeV
 $L = 5$ fm
 $\Phi_0 = 0.0$
 $\alpha = 8000^{-1}$ c/fm

Figure 9: Fermionic particle occupation numbers $\langle b_\alpha^\dagger b_\alpha \rangle$ of the individual momentum modes as a function of the dimensionless coupling constant $g_R/m = 0.04 \dots 0.64$ (0.04) and the single-particle energy ϵ_α . For coupling constants of about ≈ 0.25 a strong reduction of the single-particle energies ϵ_α – especially of the zero-momentum mode – is observed.

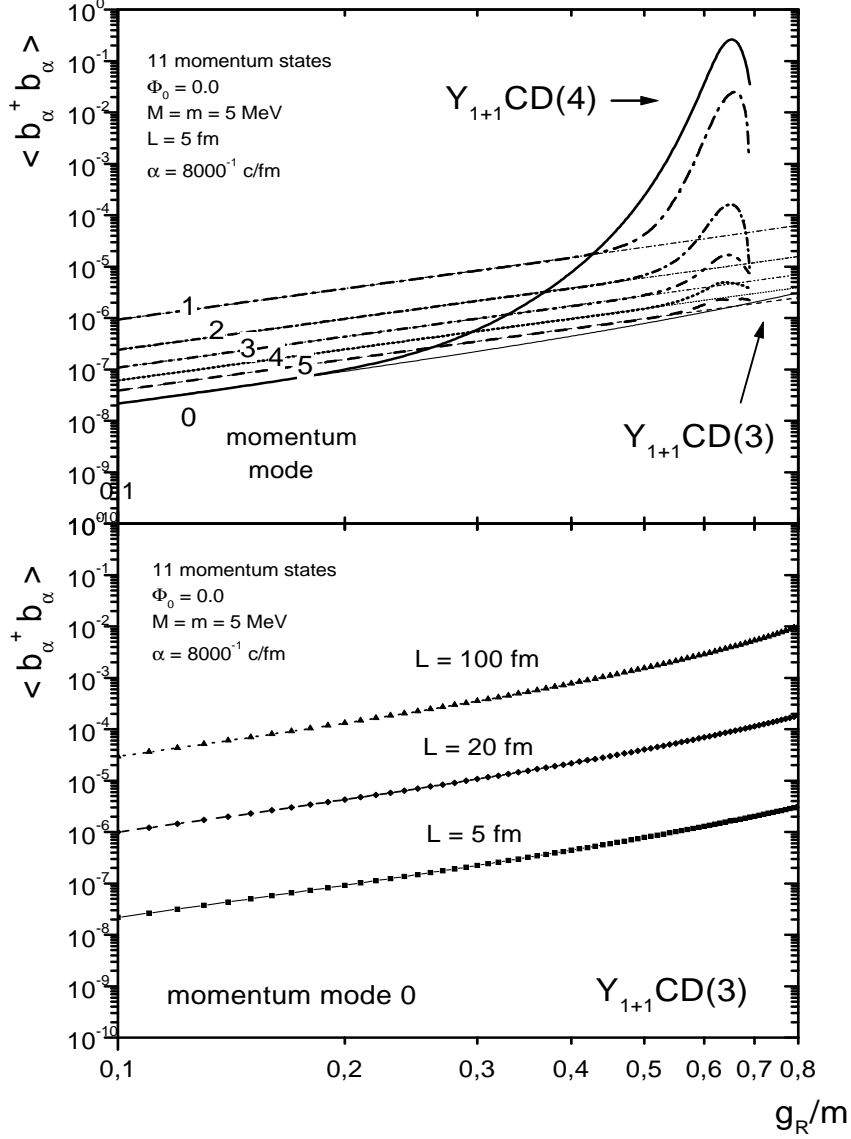


Figure 10: Occupation numbers of the individual fermionic particle modes in $Y_{1+1}CD(3)$ - and in $Y_{1+1}CD(4)$ -approximation in the small coupling regime in double logarithmic representation (upper part). Occupation number of the lowest fermionic particle mode in $Y_{1+1}CD(3)$ -approximation for various boxsizes ($L = 5$ fm, 20 fm, 100 fm) (lower part).

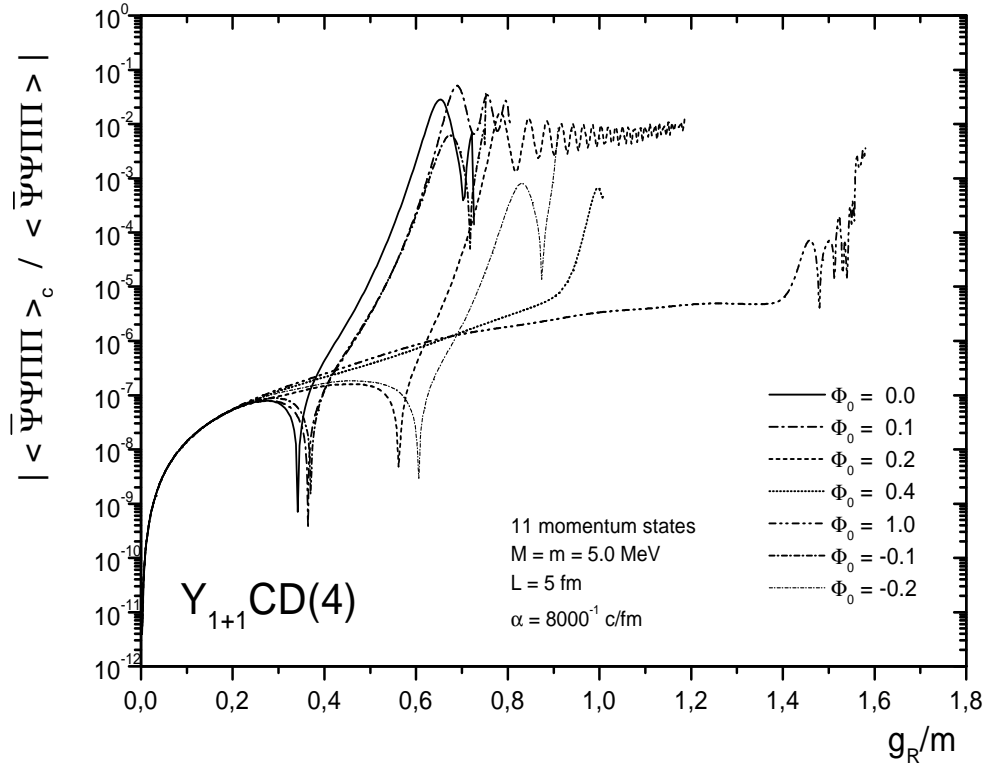


Figure 11: Correlation strength $|\langle \bar{\Psi} \Psi \Pi \Pi \rangle_c / \langle \bar{\Psi} \Psi \Pi \Pi \rangle|$ as a function of the dimensionless coupling constant g_R/m and the classical boson field Φ_0 .

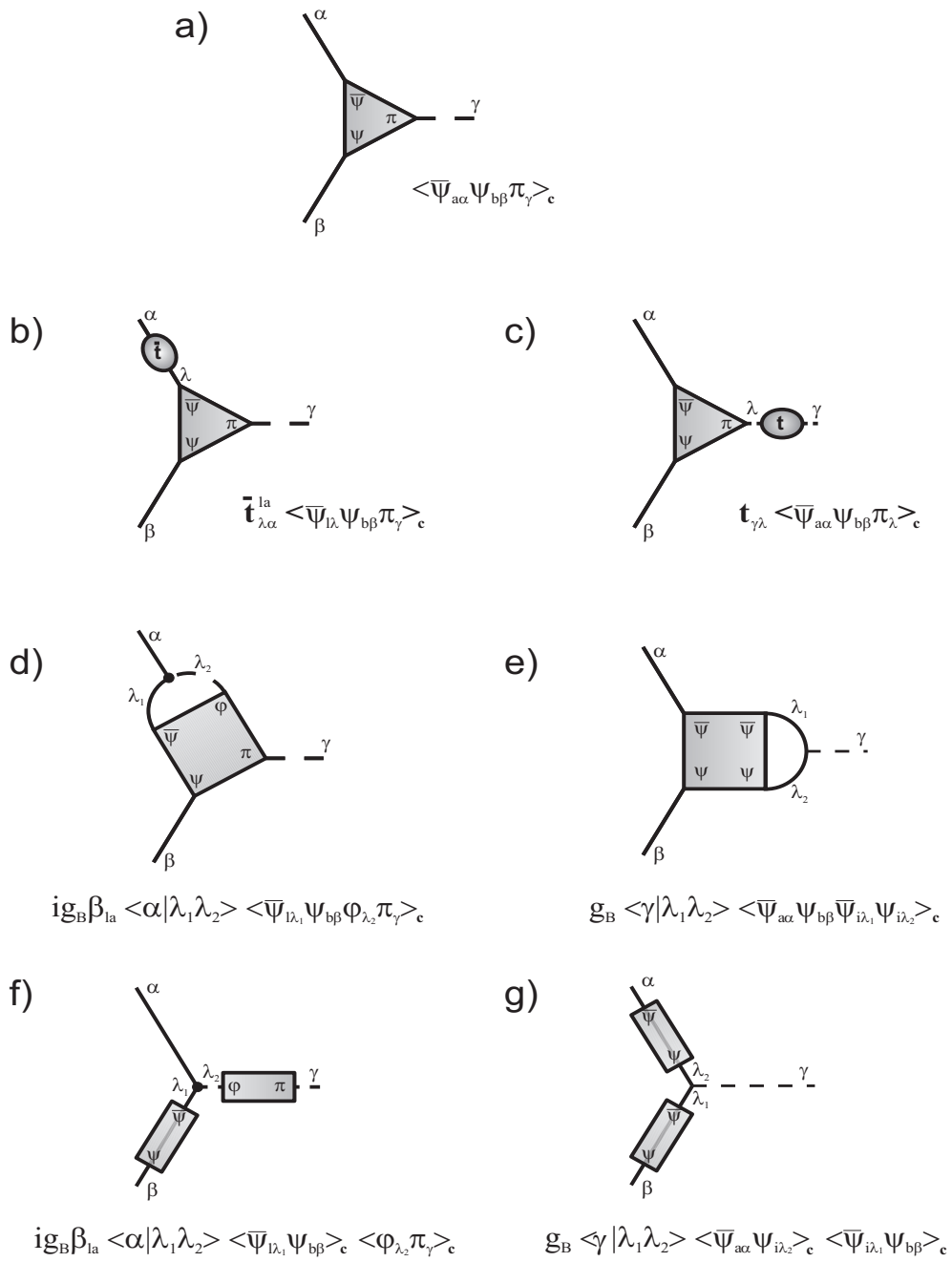


Figure 12:

Figure 12 ; Diagrammatical representation of the equation of motion for the connected equal-time 3-point function $\langle \bar{\psi}_{a\alpha} \psi_{b\beta} \pi_\gamma \rangle_c$. Connected equal-time n-point functions are represented by triangles or rectangles with a corresponding number of field-operators. The greek letters at the lines going out from the connected Green functions – fermionic lines: solid , bosonic lines: dashed – denote the momentum indices with respect to the chosen single particle basis (spinor indices are neglected for clearness). At the “vertices” momentum conservation is obeyed according to (34). Displayed are all contributions to the time evolution of $\langle \bar{\psi}_{a\alpha} \psi_{b\beta} \pi_\gamma \rangle_c$ (part a)) that arise from its $\bar{\psi}$ - (left diagrams) and π -terms (right diagrams) (cf. (75)). Parts b), c) represent contributions stemming from the free part of the Hamiltonian; the t-symbols correspond to the operators defined in (35) and (36); Parts d), e) display the coupling to connected Green functions of order n+1 introduced by the Yukawa interaction; Parts f), g) show the coupling to products of connected Green functions of lower order as a result of the cluster expansion.